DOI: 10.5327/Z2317488920140004008

ARTICLE

Geological and isotopic characteristics of granites from the Western Pernambuco-Alagoas Domain: implications for the crustal evolution of the Neoproterozoic Borborema Province

Caracterização geológica e isotópica dos granitos do Domínio Pernambuco-Alagoas Oeste: implicações na evolução crustal da Província Borborema

Rodrigo Fabiano da Cruz[1]*, Márcio Martins Pimentel[2], Ana Cláudia de Aguiar Accioly[1], Joseneusa Brilhante Rodrigues[1]

ABSTRACT: The Western Pernambuco-Alagoas Domain is a complex tectonic domain of the Southern part of the Neoproterozoic Borborema Province. It borders the Northern margin of São Francisco Craton. U-Pb and Sm-Nd data discussed in this work show that, in the Western Pernambuco-Alagoas Domain, large volumes of granitic rocks of various ages related to different tectonic events are recognized. The Cariris Velhos Event is represented by Lobo (974 ± 8 Ma) and Rocinha (956 ± 2 Ma) orthogneisses; whereas Paleoproterozoic and Archean basement rocks are represented by Fulgêncio Orthogneiss (1,996 ± 8 Ma), Riacho Seco Gneissic-migmatitic Complex (1,992 ± 27 Ma), and orthogneisses of Entremontes Complex (2,734 ± 11 Ma). Six groups of granitoids are recognized: Brasiliano granitoids (Ediacaran-Cryogenian), with Meso- to Paleoproterozoic model ages; Cariris Velhos granitoids (Tonian) yielding Mesoproterozoic model ages; Paleoproterozoic granitoids from Pernambuco-Alagoas Domain, with Neoarchean to Paleoproterozoic Nd model ages; Paleoproterozoic granitoids from Riacho Seco Nucleus, represented by Riacho Seco Gneissic-migmatitic Complex, with Archean model ages; Archean granitoids represented by the rocks of Entremontes Complex; and granitoids emplaced in the São Francisco Craton displaying Paleoproterozoic to Archean model ages. Prominent among the new data obtained is the Paleoproterozoic age of Riacho Seco Gneissic-migmatitic Complex, which is formed by Archean basement reworking. The new data reveal the presence of Paleoproterozoic and Archean basement inliers and a large volume of Cariris Velhos granitoids in the Western Pernambuco-Alagoas Domain. The orogen, therefore, involved extensive reworking of older blocks, possibly including parts of São Francisco-Congo Craton.

KEYWORDS: Neoproterozoic Orogen; U-Pb Geochronology; Sm-Nd Isotopes; Entremontes Complex; Riacho Seco Nucleus; Fulgêncio Orthogneiss.

RESUMO: *O Domínio Pernambuco-Alagoas ao Oeste é um complexo domínio tectônico na parte Sul da Província Borborema Neoproterozoica. Faz fronteira com a margem Norte do Cráton de São Francisco. Dados U-Pb e Sm-Nd deste trabalho mostram que, no Domínio Pernambuco-Alagoas Oeste, grandes volumes de rochas graníticas de várias idades, relacionados a diferentes eventos tectônicos, são reconhecidos. O Evento Cariris Velhos é representado pelos ortognaisses Lobo (974 ± 8 Ma) e Rocinha (956 ± 2 Ma); enquanto que o Ortognaisse Fulgêncio (1.996 ± 8 Ma), o Complexo Gnáissico-migmatítico Riacho Seco (1.992 ± 27 Ma) e ortognaisse do Complexo Entremontes (2.734 ± 11 Ma) representam o embasamento Paleoproterozoico e Arqueano. Seis grupos de granitoides são reconhecidos: Brasilianos (Ediacarano-Criogeniano), com idades modelo do Meso ao Paleoproterozoico; Cariris Velhos (Toniano), apresentando idades modelo mesoproterozoicas; paleoproterozoicos do Domínio Pernambuco-Alagoas, com idades modelo do Neoarqueano ao Paleoproterozoico; paleoproterozoicos do Núcleo Riacho Seco, representado por complexo gnáissico-migmatítico homônimo, com idades modelo arqueanas; arqueanos representadas pelas rochas do Complexo Entremontes; e granitoides do Cráton São Francisco, exibindo idades modelo do Arqueano ao Paleoproterozoico. Destacam-se entre os novos dados obtidos a idade paleoproterozoica do Complexo Gnáissico-migmatítico de Riacho Seco, formado pela retrabalhamento de rochas arqueanas. Os novos dados revelaram a presença de inliers de embasamento Arqueano e Paleoproterozoico e um grande volume de granitoides Cariris Velhos no Domínio Pernambuco-Alagoas Oeste. Portanto, o orógeno envolveu retrabalhamento de blocos mais antigos, possivelmente incluindo partes do Cráton São Francisco-Congo.*

PALAVRAS-CHAVE: *Orógeno Neoproterozoico; Geocronologia U-Pb; Isótopos de Sm-Nd; Complexo Entremontes; Núcleo Riacho Seco; Ortognaisse Fulgêncio.*

[1]Serviço Geológico do Brasil - SGB/CPRM, Brasília (DF), Brazil. *E-mails: rodrigo.cruz@cprm.gov.br; ana.accioly@cprm.gov.br; joseneusa.rodrigues@cprm.gov.br*

[2]Laboratório de Geocronologia, Universidade de Brasília - UnB, Brasília (DF), Brazil. *E-mail: marcio@unb.br*

*Corresponding author

Manuscrito ID: 30073. **Recebido em:** 28/12/2013. **Aprovado em:** 07/10/2014.

INTRODUCTION

The Borborema Province (Almeida *et al*. 1977), in Northeastern Brazil, underlies an area of approximately 450,000 km^2, corresponding to the Western portion of the extensive Brasiliano-Pan African orogenic system formed by a convergence of the West Africa/São Luis and San Francisco-Congo Cratons (Fig. 1). The study area is located in the Pernambuco-Alagoas Domain (PEAL) and its subdomain, the Riacho Seco Nucleus (RSN) in the Southern Borborema Province. The PEAL is located between the E-W Pernambuco Lineament to the North and the Sergipano Belt, and São Francisco Craton to the South. This is one of the crustal blocks comprising the Southern Subprovince of Van Schmus *et al*. (2011) or the Southern Domain of Brito Neves *et al*. (2000), which are part of the Neoproterozoic orogenic system along the Northern margin of São Francisco Craton.

The subdomain RSN was previously considered a small Archean block within the younger PEAL. The correlation between PEAL with other domains of the Borborema Province is still unclear, as well as the ages of their main units and tectonic events recorded in its rocks. In this study, we present U-Pb zircon ages, Nd isotopes, and geological and geochemical data of metagranites from the PEAL. Five rock units were studied and dated by U-Pb zircon dating, using Laser Ablation Inductively Coupled Plasma Mass Spectrometry (LA-ICP-MS): Entremontes Complex, Fulgêncio orthogneiss, Riacho Seco Gneissic-migmatitic Complex, Lobo and Rocinha orthogneisses. The types of analysis that each geologic unit were subjected are summarized in Tab. 1. Some isotope analyzes of the granitoids from São Francisco Craton were performed to compare with the bodies studied in the PEAL. The new data clarified several aspects of the geology of the western segment of PEAL and its role in the tectonic evolution of the Borborema Province along the Northern margin of São Francisco Craton.

ANALYTICAL PROCEDURES

Several outcrops were described and samples were collected, some of them were selected for petrographic, geochemical, and isotopic studies (Tab. 1). The most representative bodies to understand the geological setting were subjected to more detailed studies. The methodology of this study is explained as follows:

- The petrographic analysis helped defining the composition and metamorphic grade of the main units.
- Major and trace element contents were determined to establish the main group of granitoids (Entremontes Complex, Fulgêncio and Rocinha orthogneisses). Data obtained in this study were added to the geochemical ones of Salgueiro and Parnamirim Brazil Geological Service (CPRM) maps. All samples were prepared (by fusion with lithium metaborate and aqua regia digestion), and their major and trace element analyses performed by SGS Laboratories Geosol Ltda., using ICPMS technology.
- The isotopic study was the main goal of the investigation, with analyses of whole rock (Sm-Nd) and zircon grains (U-Pb). Zircon concentrates were separated from approximately five-kilogram samples. The concentration of heavy minerals was carried out by panning, which was followed by magnetic separation and final selection under a binocular microscope. Zircon grains were arranged in mounts made of epoxy resin that were polished to expose inside the grains. They were imaged using a scanning electron microscope (SEM) equipped with cathode luminescence (CL) and backscattered electron (BSE) detectors in order to select the best spots for mineral analyses. The U-Pb evaluations were carried out with a Thermo-Finnigan multi-collector LA-ICP-MS installed at the Geochronology Laboratory of University of Brasília (samples RF-111, RF-243 and RF-270) and at the Laboratory of Isotope Geology of the Federal University of Rio Grande do Sul (samples RF-179 and RF-323). Ages were calculated using the ISOPLOT 3.0 software (Ludwig 2000). Twenty to 40 spot analyses were carried out for each sample. The Sm-Nd isotopic analyses were performed at both mentioned university laboratories and both followed the method described by Gioia and Pimentel (2000). In this procedure, approximately 50 mg of the sample is mixed with a powdered tracer solution (^{149}Sm and ^{150}Nd), then dissolved by repeated acid attacks. Sm and Nd are extracted using cationic exchange columns. Purified aliquots of Sm and Nd are deposited on Re filaments. Isotopic analyses were carried out by Thermal Ionization Mass Spectrometry (TIM). Instrument fractionation on ^{143}Nd/^{144}Nd ratios was corrected applying the ^{146}Nd/^{144}Nd ratio of 0.7219. The T_{DM} values were calculated using De Paolo's model (1981).

BORBOREMA PROVINCE

Borborema Province (Almeida 1967; Almeida *et al*. 1977) consists of a mosaic of tectonic blocks including varied proportions of Paleoproterozoic basement and scattered Archean nuclei, Meso- to Neoproterozoic supracrustal rocks, and large intrusions of granitic rocks emplaced during the Neoproterozoic Brasiliano orogen, in 650 to 580 Ma (Van Schmus *et al*. 2008; Brito Neves *et al*. 2000). The Neoproterozoic evolution of the Borborema Province took place during the West Gondwana agglutination

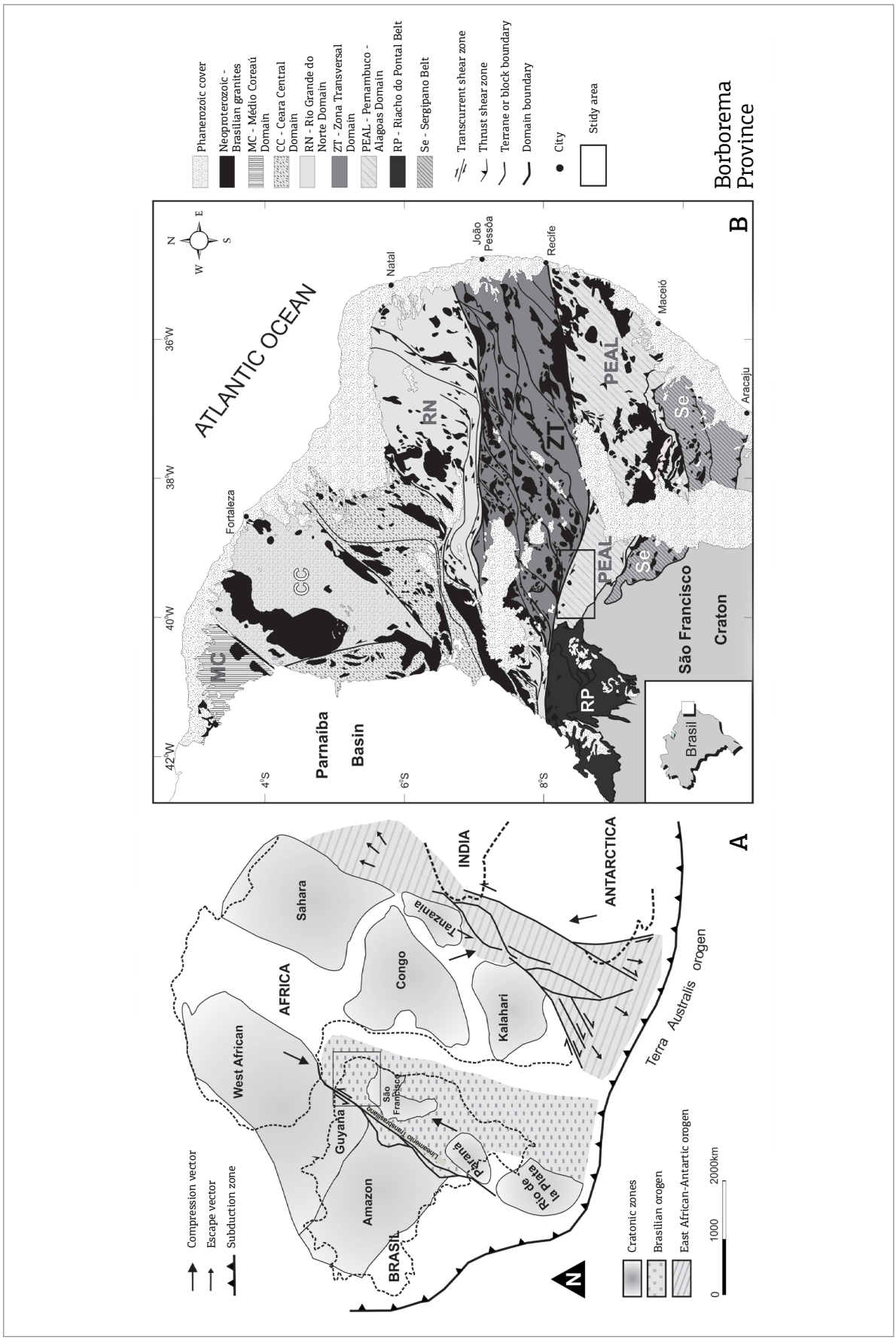

Figure 1. (A) Orogenic belts of Western Gondwana 650 Ma ago, modified from Teixeira *et al.* (2010); (B) Borborema Province and its geotectonic domains, modified from Medeiros (2004).

Table 1. Summary of samples collected.

Unit	Point	Coord_X	Coord_Y	Chemistry	Sm-Nd	U-Pb
Brasiliano granites						
Ibó Migmatite	RF022	471224	9045282		x	
Ibó Migmatite	RF068	463255	9029986		x	
Chorrochó Augen-gneiss	RF027	471119	9033550		x	
Bendó Orthogneiss	RF415	443316	9082776		x	
	RF322	438801	9069760		x	
Cariris Velhos granites						
Lobo Orthogneiss	RF270	472784	9069820		x	x
Rocinha Orthogneiss	RF010	488055	9048504		x	
Rocinha Orthogneiss	RF033	466796	9041103	x	x	
Rocinha Orthogneiss	RF311	432497	9072305	x		
Rocinha Orthogneiss	RF323	439101	9068004	x	x	x
Rocinha Orthogneiss	RF323B	438698	9068243	x		
Rocinha Orthogneiss	RF323C	439368	9067372	x		
Rocinha Orthogneiss	RF466	439784	9067173	x		
Rocinha Orthogneiss	RF467	440177	9066216	x		
Rocinha Orthogneiss	FL180	447512	9077182	x		
Rocinha Orthogneiss	FL181	446766	9077557	x		
Rocinha Orthogneiss	SF182	447364	9075216	x		
Rocinha Orthogneiss	FL185	446365	9073209	x		
	RF003	472752	9056286		x	
Paleoproterozoic granites						
Fulgêncio Orthogneiss	RF040	450613	9045530	x	x	
Fulgêncio Orthogneiss	RF240	417807	9050234	x		
Fulgêncio Orthogneiss	RF241	416630	9052437	x		
Fulgêncio Orthogneiss	RF242	415278	9052878	x		
Fulgêncio Orthogneiss	RF243	415448	9055151	x	x	x
Fulgêncio Orthogneiss	RF244	413205	9057996	x	x	
Fulgêncio Orthogneiss	RF267	415503	9068278	x	x	
Fulgêncio Orthogneiss	RF287	413833	9067886	x		
Fulgêncio Orthogneiss	RF288	415434	9067893	x		
Fulgêncio Orthogneiss	RF289	416240	9067910	x		
Fulgêncio Orthogneiss	RF292	452458	9065471	x		
Fulgêncio Orthogneiss	RF328	415508	9069694	x		
Fulgêncio Orthogneiss	RF579	411536	9060713	x		
RSGMC*	RF111	434681	9037013		x	x
RSGMC*	RF136	426457	9031204		x	
Caraíbas Migmatite	RF128	430882	9042347		x	
Caraíbas Migmatite	RF249	424686	9044946		x	
SFCG**	RF171	422407	9029967		x	
SFCG**	RF261	400890	9026667		x	
	RF165	447126	9051506		x	
Archean granites						
Entremontes Complex	RF179	400755	9090278	x	x	x
Entremontes Complex	RF262	396905	9072702	x		
Entremontes Complex	RF403	391342	9084593	x		
Entremontes Complex	RF425	400081	9089589	x		
Entremontes Complex	RF454	418990	9088526	x		
Entremontes Complex	RF503	391666	9089173	x		

(Trompette 1994). In paleogeographic reconstructions, the province extends from Central and Northeastern Brazil to West Africa through the Neoproterozoic orogenic areas of Cameroon, Nigeria, Niger, Algeria, Togo, and Benin (Fig. 1). This Province includes a complex system of high-temperature crustal scale shear zones that separate the province into tectonic domains, and they also control the emplacement of granites during the Brasiliano/Pan-African orogeny (Caby *et al*. 1991; Jardim de Sá 1994; Vauchez *et al*. 1995).

The province has been studied for decades, and different authors developed evolution models and configuration of their different domains (Almeida *et al*. 1981; Brito Neves 1983; Brito Neves *et al*. 1982, 2000; Jardim de Sá 1994; Sial 1986; Neves 2003; Silva Filho *et al.* 2002; Santos *et al*. 2010; Van Schmus *et al*. 1995, 2011; Ganade de Araújo *et al*. 2014. In this paper, the internal divisions of the Borborema Province used are based on models put forward by Van Schmus *et al*. (1995, 2008), Brito Neves *et al*. (2000) and Santos *et al*. (2000, 2010). They subdivided the province into three sub-provinces (Fig 1):

- Northern, including Médio Coreaú, Ceará Central and Rio Grande do Norte domains;
- Central (or Transversal Zone) with Piancó-Alto Brígida, Alto Pajeú, Alto Moxotó and Rio Capibaribe domains or terranes, and
- Southern or External, including Riacho do Pontal, Pernambuco-Alagoas and Sergipano domains.

The Northern Sub-province is exposed to the North of Patos Shear Zone, and consists mainly of Paleoproterozoic basement (including some Archean nuclei) partially covered by Neoproterozoic supracrustal rocks and intruded by Brasiliano plutonic rocks. The Central Sub-province is exposed between Patos and Pernambuco shear zones, and it is mainly characterized by the NE-SW to EW transcurrent faults system. The Southern Sub-province, confined between Pernambuco Shear Zone and São Francisco Craton, includes Sergipano and Riacho do Pontal supracrustal belts and Pernambuco-Alagoas Domain, which can be divided into Western and Eastern segments, separated by Tucano-Jatobá Cretaceous sedimentary basin (Angelim & Kosin 2001), as seen in Fig. 1.

Main tectonic domains and events

Archean and Paleoproterozoic rock units

Archean rock units are not widespread in Borborema Province and they form small inliers or nuclei among Paleoproterozoic terrains, such as São José do Campestre Massif comprising rocks with U-Pb zircon ages between 3.4 and 2.7 Ga (Dantas *et al*. 1998; 2004); Troia-Pedra Branca Block, where orthogneisses of Cruzeta Complex gave U-Pb zircon ages between 2.85 and 2.64 Ga (Fetter 2000); and Entremontes Complex with orthogneiss dated by U-Pb zircon data as 2.734 ± 11 Ga (Cruz 2013). Paleoproterozoic basement in the Borborema Province includes rocks formed during three major events, with ages at 2.35, 2.15 and 2.0 Ga (Dantas 1997; Neves *et al*. 2006; Souza *et al*. 2007). On the African counterpart (Congo Craton), Lerouge *et al*. (2006) have reported SHRIMP U-Pb zircon ages of 2,066 and 2,044 Ma for the emplacement of granitoids and of ca. 2050 and 1985 Ma for metamorphic events. These ages from African and South-American counterparts represent a segment of the Eburnean–Trans-Amazonian orogeny that resulted in the formation of a possible Paleoproterozoic supercontinent.

Cariris Velhos Event

Additionally to the Paleoproterozoic tectonic events, rocks that form Borborema Province were also affected by Cariris Velhos (1.0 – 0.9 Ga) and Brasiliano events (650 – 580 Ma). The Cariris Velhos Belt consists of augen gneisses, metasedimentary and metavolcanic rocks (felsic and mafic). Kozuch (2003), Brito and Cruz (2009), Santos *et al*. (2010) and Van Schmus *et al*. (2010) have constrained Cariris Velhos Event between 990 and 940 Ma, based on SHRIMP U-Pb in detrital zircon grains from metasedimentary rocks, as well as on TIMS and LA-ICPMS U-Pb data of orthogneiss and volcanic rocks.

The Cariris Velhos Event (Santos 1995) was originally defined as an orogenic event forming an extensive metamorphic belt, inserted within Alto Pajeú Domain (Brito Neves *et al*. 1995; Santos *et al*. 2010). Other authors (Bittar 1998; Neves 2003) argue, however, that Cariris Velhos Event represents an extensional event associated with continental rifting, which formed rocks dated between 1.0 and 0.9 Ga. This latter interpretation was based on the geochemical nature of volcanic and plutonic rocks, as well as on the absence of metamorphic zircon ages in the range between 1.0 and 0.9 Ga.

Brasiliano Orogeny

The Brasiliano Orogeny (650 – 500 Ma) affected the whole Borborema Province and was responsible for the regional deformation and medium- to high-grade metamorphism, for the generation and emplacement of large volumes of granite throughout the province, and also for the development of continental-scale transcurrent shear zones, which is one of the main characteristics of the province. Two main models have been used to describe the geodynamic evolution of Borborema Province during the Neoproterozoic. In one of them, the Borborema Province is considered the product of an accretionary event involving the collage of several allochthonous terrains (Brito Neves *et al*. 2000; Santos *et al*. 2004). The other

model suggests an intra-plate setting in which reworking of pre-existing Archean-Paleoproterozoic crust and deposition of Proterozoic volcano-sedimentary sequences took place in an intra-continental environment (Neves 2003; Neves *et al*. 2014; 2006). A new model proposed by Ganade de Araújo *et al*. (2014), based on some aspects of the mentioned ones, suggests that the Borborema Province underwent two major collisional events, one between 620 and 610 Ma and another between 590 and 580 Ma.

Brasiliano magmatism

The Brasiliano magmatism is symbolized by a series of granitoids with different types and dimensions. Most of the Neoproterozoic granite genesis is coeval with the development of large shear zones, which exerted strong tectonic control on the emplacement of the granitoids (Caby *et al*. 1991; Vauchez *et al*. 1995). The older Neoproterozoic plutons (640 – 610 Ma) are more strongly deformed, suggesting the pre- to syn-tectonic nature of intrusions. Younger plutons (590 – 570 Ma), on the other hand, are mostly undeformed and are therefore considered to be late- to post-tectonic intrusions. All schemes of classification of the Neoproterozoic granitic magmatism in NE Brazil (e.g. Almeida *et al*. 1977; Sial 1986; Guimarães *et al*. 1998) describe the increasing alkalinity of the magmatism with time, starting with normal calc-alkaline rocks and ending with alkali-rich granites and shoshonites. The most recent classification is from Van Schmus *et al*. (2011), who recognized five stages: Phase I, consisting of pre-collisional granitoids (650 – 610 Ma); Phase II, syn-collisional granites (610 – 595 Ma); Phase III, post-collisional, pre-transcurrent granites (595 – 576 Ma); Phase IV, syn-transcurrent intrusions (576 – 560 Ma); and Phase V, post-tectonic granites (550 – 530 Ma).

Western Pernambuco-Alagoas Domain

The PEAL is an East-West oriented tectono-stratigraphic block of the Southern part of Borborema Province (Van Schmus *et al*. 2008). It was originally defined as a massif formed by Archean to Paleoproterozoic gneisses and migmatites, intruded by Brasiliano granitic bodies (Brito Neves *et al*. 1982). PEAL (Fig. 2) is now considered a complex tectonic domain including units of various ages (Van Schmus *et al*. 1995; Silva Filho *et al*. 2002; Oliveira *et al*. 2006; Cruz 2013; Cruz *et al*. In press). Two main units in the Western segment of the domain are recognized (Santos 1995; Medeiros & Santos 1998; Medeiros 2000): Cabrobó Complex comprising metavolcanosedimentary and metasedimentary sequences metamorphosed under amphibolite facies conditions, with local migmatites, and Belém do São Francisco Complex formed mainly by granitic-granodioritic gneisses and migmatites with remnants of supracrustal rocks and mafic lenses. U-Pb dating on zircon of granodiorite gneiss of Belém do São Francisco Complex indicated the age of 2,074 ± 34 Ma (Silva *et al*. 2002).

The metamorphic complexes of PEAL are intruded by variably deformed pre- to post-tectonic Neoproterozoic plutonic rocks. Recent U-Pb zircon data produced during mapping projects of the Brazilian Geological Survey, as well as by the present work suggest that Belém do São Francisco Complex may be divided into different units: Neoarchean Entremontes Complex, Orosirian Fulgêncio Orthogneiss, and Lobo and Rocinha orthogneisses related to Tonian Cariris Velhos Event. Besides the wide range of ages found in PEAL rocks, the structural complexity of the area is also noteworthy with thrust sheets in contact with São Francisco Craton and Sergipano and Riacho do Pontal belts. Transcurrent zones along the contact with the Transversal Zone to the North are recognized.

The RSN (Santos 1995; Angelim & Kosin 2001) has been considered the exposure of older (Archean) rock units enclosed within PEAL. It may be subdivided into two major units (Cruz *et al*. In press): Riacho Seco Gneissic-migmatitic Complex that is made up of gneissic rocks, generally migmatized, including remnants of medium- to high-grade supracrustal rocks, and Riacho Seco Metasedimentary Complex represented by schists and gneisses of medium to high metamorphic grade, calcium-silicates rocks, and marbles. A Rb-Sr isochron on migmatites indicates an age of 2.9 Ga for these rocks (Mascarenhas & Garcia 1989), whereas a Sm-Nd (T_{DM}) model age for Riacho Seco orthogneisses is ca. 3.1 Ga (Angelim & Kosin 2001). Both ages suggest an overall Archean age for the RSN rocks. Such nucleus is partially surrounded by the Cabrobó Complex along a contractional shear zone. In the South, it is in contact with São Francisco Craton through the sinistral transcurrent Riacho Seco Shear Zone.

Archean granitoids

Entremontes Complex

The Entremontes Complex (Cruz 2013) consists mainly of granitic and minor granodioritic gneisses, as well as of some local amphibolite outcrops. The petrographic analyses of the granitic gneiss show that the main mafic mineral is amphibole (hornblende and hastingsite), followed by biotite, and minor garnet and clinopyroxene (hedenbergite). Migmatism and compositional banding are common, as well as milonitic structures as mineral stretching. The metamorphic conditions reached the medium grade (recrystallization of K-feldspar+biotite+amphibolite), with retrogression to lower grade (biotite recrystallized). The geochemical analyzes resulted in high SiO_2 contents (74 to 70%), as

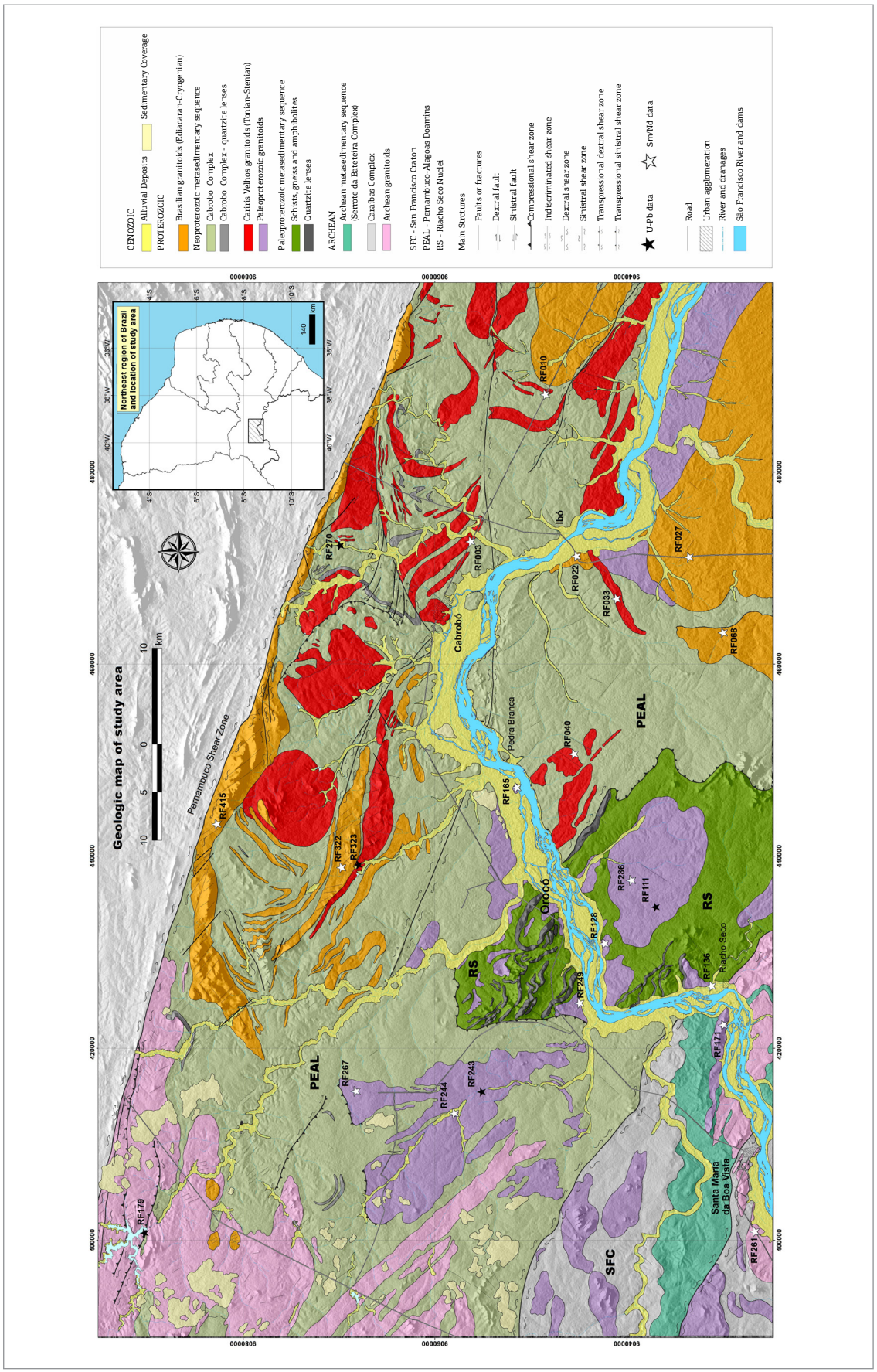

Figure 2. Simplified geological map of the study area with sample locations. The map covers a large area of Western Pernambuco-Alagoas Domain (PEAL) and a small portion of the São Francisco Craton in the SW of the study area. The sample references and unit names are: RF179 -Entremontes Complex (Archean Granitoids); RF111 – Riacho Seco Gneissic-migmatitic Complex and RF243 – Fulgêncio Orthogneiss (Paleoproterozoic granitoids); RF323 –Rocinha Orthogneiss and RF270 – Lobo Orthogneiss (Cariris Velhos granitoids).

seen in Tab. 2, and metaluminous to peraluminous high-K calc-alkaline to alkaline compositions (Figs. 3A to 3C). In chondrite-normalized REE diagram (Boynton 1984), the patterns show fractionation between HREE and LREE and negative Eu anomalies (Fig. 4A). The primordial mantle normalized spidergram (Wood *et al.* 1979) presents negative anomalies of Ba, Nb, Ta, U, and Sr as well as strong negative Ti anomaly and marked enrichment in Tb and Y (Fig. 4D), some of these characteristics are also viewed in the ORG normalized spidergram (Pearce 1984), as seen in Fig. 4G. In Pearce's (1994) diagram (Fig. 5A), samples fall in the post-collisional to intra-plate field and according to the criteria (A1/A2) established by Eby (1992), they fall in the WPG+ORG and A2 field, indicative of A-type granites derived from mixed sources (Figs. 5B to 5D). The Entremontes Complex, as indicated by chemical data, is related to A-type magmatism most likely in a post-collisional setting.

Paleoproterozoic granitoids

Paleoproterozoic granites of PEAL in the studied area include granitic migmatites and orthogneisses found in the vicinities of Orocó, Pernambuco State (Orocó Migmatites), and Fulgêncio Orthogneisses; those from RSN comprising granitic migmatite exposed along São Francisco River near Orocó city, Pernambuco state (Caraíbas migmatites), and Riacho Seco Gneissic-migmatitic Complex; and São Francisco Craton granitoids including a pink alkaline migmatite near Riacho Seco and a biotite gneiss with sillimanite and garnet found near Santa Maria da Boa Vista, Pernambuco.

Fulgêncio Orthogneiss

This is a porphyroblastic coarse-grained migmatitic orthogneiss that contains discontinuous bands of concentrations of feldspar augen. In outcrops located to the South, the augen texture predominates, and structures like banding are scarce. Other structural features are shear bands with predominant dextral sense, mineral stretching lineation oriented North to South and low-to medium-angle foliation dipping to the West. Biotite is the main mafic mineral, accessory minerals are apatite, titanite, zircon, allanite, and opaque minerals. The recrystallization of K-feldspar and presence of metamorphic amphibole indicate upper greenschist to amphibolite facies, with retrogression to greenschist facies indicated by biotite recrystallization. An additional petrographic facies of these orthogneisses is found at the NW portion of the exposure area, consisting of fine-grained banded rocks. Inter-fingering of the two textural facies was found in some outcrops.

The geochemical analyzes show SiO_2 contents ranging between 65 and 74% (Tab. 3) and present high-K calc-alkaline and metaluminous to peraluminous nature (Figs. 3A to 3C). The REE diagram (Boyton 1984), as seen in Fig. 4B, shows strong fractionation between LREE and HREE and negative Eu anomalies. In the primordial mantle-normalized spidergram (Wood *et al.* 1979), as in Fig. 4E, negative anomalies of Ba, Nb, U, Ti and Y are observed, some of them are also seen in the ORG normalized spidergram (Pearce *et al.* 1984), Fig. 4H, suggesting the presence of subduction-related metasomatized mantle in their genesis. Very low concentrations of Sr indicate a marked fractionation of plagioclase in the original magma. In the tectonic discrimination diagram of Pearce *et al.* (1994), Fig. 5A, these samples correspond to post-collisional granitic composition, close to the boundary between syn-collisional and volcanic arc granite fields. In Eby (1992) diagrams, the samples demonstrate characteristics of late- to post-collisional tectonic setting with a probably mixed magma source (Figs. 5B to 5D).

Riacho Seco Gneissic-migmatitic Complex

This complex consists of orthogneisses with remnants of supracrustal rocks. It comprises the basement rocks of RSN, in this subdomain the supracrustal sequence is represented by Riacho Seco Metasedimentary Complex. The main rock types identified are reddish granitic orthogneiss with biotite and subordinately granodioritic orthogneiss with titanite and hornblende. They show subtle to well-developed compositional banding by different proportions of mafic minerals. Some outcrops are migmatitic locally mafic gneisses and amphibolite lenses are also present. Mineral textures (K-feldspar porphyroblasts) and paragenesis (recrystallized K-feldspar+biotite+amphibole) seen in the felsic gneisses suggest an amphibolite-facies metamorphism. The garnet-diopside-amphibole paragenesis, locally recognized, suggests that the unit might have reached the granulite facies with subsequent retrogression to amphibolite/upper greenschist facies.

Cariris Velhos granitoids

The Cariris Velhos granites (Tonian-Stenian) are represented by a migmatized granite body near to Cabrobó city in Pernambuco state (Cabrobó migmatite), and also by Lobo and Rocinha orthogneisses.

Lobo Orthogneiss

Lobo Orthogneiss defined by Brito and Freitas (2011) comprises medium- to fine-grained

Table 2. Geochemical data from Entremontes Complex.

	Entremontes Complex					
SAMPLE	**RF-425**	**RF-179**	**RF-503**	**RF-454**	**RF-262**	**RF-403**
Wt %						
SiO_2	72.55	71.55	71.78	73.66	73.41	71.49
TiO_2	0.26	0.3	0.41	0.34	0.38	0.49
Al_2O_3	11.43	11.82	11.75	11.37	11.77	11.91
Fe_2O_3	3.25	3.85	4.9	4.25	4	4.58
CaO	0.9	1.2	1.3	1	0.98	1.55
Cr_2O_3	< 0.01	< 0.01	< 0.01	< 0.01	< 0.01	< 0.01
K_2O	6.35	6.13	4.3	4.9	5.31	5.3
MgO	0.09	0.26	0.13	0.26	0.12	0.39
MnO	0.05	0.05	0.08	0.08	0.07	0.08
Na_2O	2.44	2.69	2.96	2.76	2.69	0.33
P_2O_5	0.06	0.1	0.03	0.04	< 0.01	0.06
Sum	< 0.01	< 0.01	0.08	0.1	0.06	0.04
LOI	97.38	97.89	97.71	98.75	98.79	96.21
ppm						
Ba	613	742	994	1026	884	883
Be	3.2	3.4	4	0.4	3.2	0.4
Cs	0.18	0.06	0.22	0.34	< 0.05	0.18
Ga	21.4	19.4	23.5	22.1	26.6	21.9
Hf	13.69	13.36	16.01	17.72	17	13.79
Nb	28.7	25.03	24.29	19.46	30.04	31.07
Rb	162	144	137	164	160	162
Sn	8.4	6.3	4.9	6.3	4.1	3.9
Sr	52.9	77.6	95.6	70.3	62.5	77
Ta	2.09	2.87	1.34	1.39	1.02	1.65
Th	33.9	20.5	15.3	19	27.3	15.1
U	1.58	1.95	1.62	1.94	1.69	1.64
W	2.2	0.2	0.9	1.2	< 0.1	< 0.1
Y	71.17	67.82	63.14	84.57	84.23	69.74
Zr	521	597	657	629	547	554
Ag	0.02	0.03	0.08	0.11	0.1	< 0.01
Au	< 0.1	< 0.1	< 0.1	< 0.1	< 0.1	< 0.1
As	< 1	< 1	< 1	< 1	< 1	2
Bi	< 0.02	< 0.02	< 0.02	< 0.02	< 0.02	< 0.02
Cd	0.06	0.02	0.11	0.09	0.09	0.04
Co	1	1.4	1.7	2.7	1.7	3.6
Cu	3.8	3.1	9.1	11.3	3.9	15.4
Hg	< 0.01	< 0.01	< 0.01	0.05	0.01	0.02
Mo	0.45	1.9	2.86	1.34	2.09	2.95
Ni	1.9	1.2	6	2	1	3.7
Pb	2.6	1.8	2.2	5.4	3.7	3.4
Sb	< 0.05	< 0.05	< 0.05	< 0.05	< 0.05	< 0.05
Se	< 1	< 1	2	3	< 1	2
Zn	41	31	53	67	70	43
Ce	224.7	170.4	194.9	224.3	222.5	199.5
Dy	15.27	13.55	13.18	17.84	15.18	13.47
Er	8.02	7.25	7.22	9.25	8.31	8.95
Eu	1.69	1.82	2.4	3.51	1.73	2.68
Gd	15.62	14.25	14.82	24.65	16.59	19.41
Ho	2.89	2.62	2.73	3.17	2.9	2.72
La	119.6	105.6	89	136.2	116.4	102.7
Lu	0.99	0.97	0.96	1.25	< 0.05	1.18
Nd	86.7	74.1	85.3	115.5	95.1	89.9
Pr	24.29	20.55	22.79	29.66	26.38	24.44
Sm	16.3	13.7	16.7	19.6	17.7	14.1
Tb	2.56	2.22	2.19	3.54	2.32	2.64
Tm	1.16	1.14	0.91	1.38	1.02	1.12
Yb	7.2	7.3	6.4	7.5	7.5	7.5

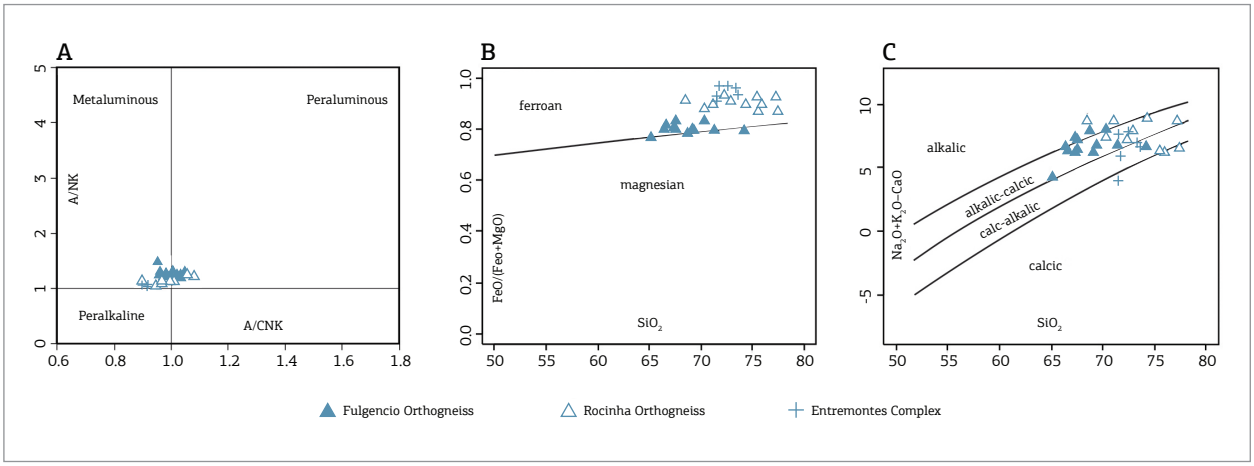

Figure 3. Lithogeochemical diagrams: (A) Diagram A/CNK *versus* A/NK (Shand 1943); (B and C) Major-element diagrams based on classification of granitoids (Frost *et al.* 2001).

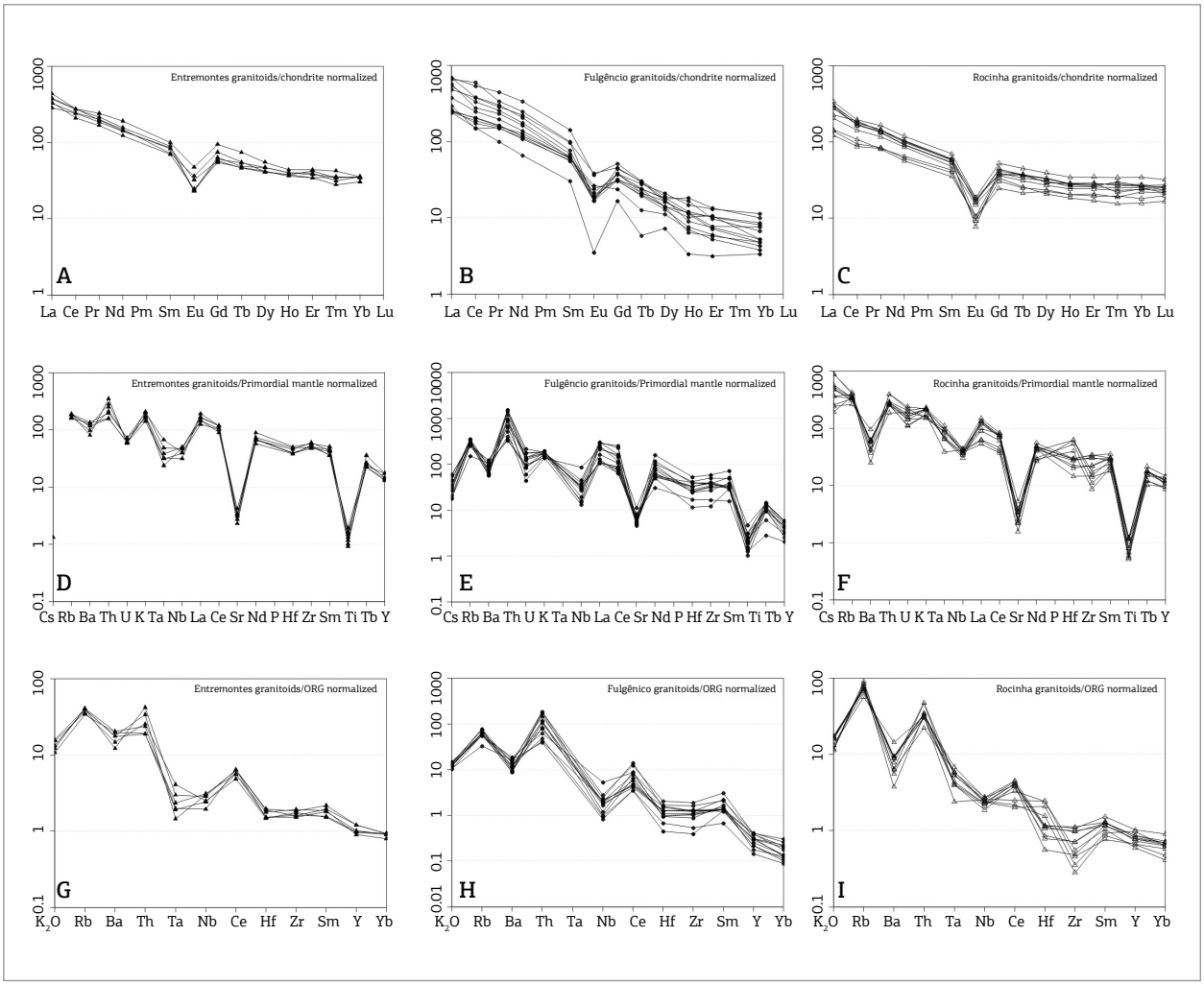

Figure 4. Multi-elemental diagrams: (A to C) REE diagrams (Boynton 1984); (D to F) Expanded diagrams normalized by primordial mantle (Wood *et al.* 1979); (G to I) Expanded diagrams normalized by ORG (Pearce *et al.* 1984) in order – Entremontes Complex, Fulgêncio Orthogneiss, and Rocinha Orthogneiss samples.

garnet-muscovite-biotite granitic to granodioritic orthogneisses, locally containing K-feldspar augens and mafic xenoliths. They exhibit low angle foliation, with mineral stretching lineation generally oblique or perpendicular to the foliation plane. Metamorphic conditions were of the upper greenschist facies indicated by the presence of K-feldspar and biotite recrystallized and garnet. Compositionally, it is metaluminous to peraluminous and of medium-K calcalkaline nature.

Rocinha Orthogneiss

Rocinha Orthogneiss established by Cruz and Accioly (2013) consists of coarse- to medium-grained porphyroclastic to porphyroblastic granite, and the main mafic mineral is biotite, commonly displaying mylonitic features and metamorphosed under upper greenschist- to amphibolite-facies conditions indicated by deformation and recrystallization of K-feldspar and biotite. The geochemical analyzes show high SiO_2 (Tab. 4) contents (77 to 68%), K calc-alkaline to alkaline nature and metaluminous to slightly peraluminous chemical characteristics (Figs. 3A to 3C). Patterns in the primordial mantle-normalized (Wood *et al.* 1979) multi-element diagram (Fig. 4F) presents negative Nb anomalies, characteristically found in magmas sources modified by subduction, and also pronounced negative Sr and Ti anomalies and Tb and Y enrichment, a Ta-Nb depletion is observed in the Ocean Ridge Granites (ORG) -normalized spidergram (Pearce *et al.* 1984), as in Fig. 4I. The chondrite-normalized REE diagram (Boynton 1984), Fig. 4C, reveals flat HREE patterns and strong negative Eu anomalies, which are features similar to those of rocks formed in intra-plate settings. In the trace element diagrams of Pearce (1996) and Eby (1992), Figs. 5A to 5D, these rocks are similar to post-collisional/intra-plate rocks and A-type (A2) granites. The chemical signatures of Rocinha Orthogneiss suggest that the original magmas were formed in a post-collisional setting.

Brasiliano granitoids

Some additional granite bodies correlated to the Brasiliano Cycle were investigated in this study: Cryogenian-Ediacaran intrusions, among these are the equigranular medium- to fine-grained with muscovite-biotite or biotite-amphibole migmatitic granitic body with metasedimentary xenoliths exposed in Ibó, in Bahia state (Ibó migmatites); and the grey amphibole-biotite granitic augen-gneiss of Chorrochó and Abaré, Bahia state (Chorrochó augen-gneiss).

ISOTOPIC DATA

U-Pb Data

New U-Pb data were acquired for this investigation. The results were used in combination with data obtained for the Salgueiro and Parnamirim mapping projects carried out by the Brazilian Geological Survey (CPRM) and they are available at http://geobank.sa.cprm.gov.br.

Entremontes Complex

The zircon grains from the sample of amphibole -bearing granitic gneiss dated in this study (RF-179 – Tab. 5) are prismatic with rounded edges, and they have an average aspect ratio of 3:1 (Fig. 6A). Many grains are strongly fractured and have abundant inclusion, thus rendering them not suitable for analysis. Some grains show subtle concentric or irregular zoning, and in others overgrowths and cores are recognized. A few grains of

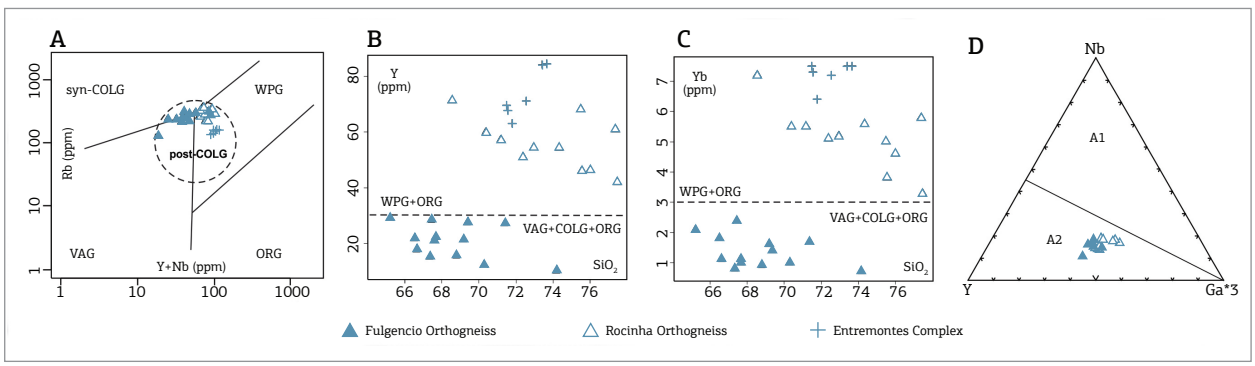

Figure 5. Lithogeochemical plots: (A) Geotectonic setting classification diagram by Pearce (1996); (B and C) by Eby (1992). Discriminate diagram of A-type granitoids (Eby 1992).

Table 3. Geochemical data from Fulgêncio Orthogneiss.

	Fulgêncio Orthogneiss							
SAMPLE	**RF-287**	**RF-288**	**RF-289**	**RF-328**	**RF-267**	**RF-292**	**RF-240**	**RF-241**
Wt %								
SiO_2	66.64	68.78	66.51	71.39	70.28	67.44	69.36	65.19
TiO_2	0.49	0.26	0.57	0.4	0.36	0.54	0.79	1.19
Al_2O_3	13.36	14.83	13.45	12.91	13.86	13.63	15.14	14.84
Fe_2O_3	3.55	2.4	4.56	3.03	2.86	3.93	5.14	6.15
CaO	1.74	1.32	1.7	1.3	0.98	1.33	2	3.09
Cr_2O_3	< 0.01	< 0.01	< 0.01	< 0.01	< 0.01	< 0.01	< 0.01	< 0.01
K_2O	5.04	5.88	5.44	5.07	5.96	5.59	5.32	4.12
MgO	0.72	0.58	1	0.69	0.5	0.83	1.18	1.7
MnO	0.04	0.03	0.06	0.03	0.03	0.04	0.06	0.08
Na_2O	3.08	3.45	2.92	2.96	3.14	3.21	3.51	3.36
P_2O_5	0.2	0.09	0.08	< 0.01	0.07	0.14	0.38	0.4
Sum	0.19	0.21	0.12	0.37	0.13	0.25	0.38	0.38
LOI	95.07	97.82	96.41	98.14	98.17	96.93	103.28	100.52
ppm								
Ba	436	616	477	557	437	495	709	932
Be	1.5	1.6	2.4	2.3	2	1.4	6.4	3.3
Cs	0.52	0.51	0.69	0.4	0.58	0.83	0.87	1.15
Ga	21	19.1	20.9	17.7	19.7	20.1	23.8	24.9
Hf	9.77	4.04	11.27	8.77	8.54	8.96	18.36	14.8
Nb	20.17	9.31	17.91	9.86	11.94	18.87	28.04	53.26
Rb	250	242	304	217	246	291	305.6	223.1
Sn	2.6	4.3	7.2	1.9	3.4	3.3	1.4	3.3
Sr	117	163	116	132	104	115	152.1	257.1
Ta	1.09	0.45	1.09	0.69	0.86	1.55	0.94	1.37
Th	84.2	38.3	147.1	93.7	134.9	66.1	146.5	49.9
U	3.91	2.25	5.83	3.37	3.83	4.83	4.72	1.19
W	< 0.1	< 0.1	2.6	< 0.1	< 0.1	0.6	1.2	0.1
Y	17.56	15.35	21.66	27.03	12.38	28.23	27.46	29.14
Zr	374	133	432	347	298	355	648.4	552.3
Ag	0.02	0.02	0.05	< 0.01	0.06	0.01	< 0.01	< 0.01
Au	< 0.1	< 0.1	< 0.1	< 0.1	< 0.1	< 0.1	< 0.1	< 0.1
As	< 1	< 1	< 1	< 1	< 1	< 1	2	< 1
Bi	< 0.02	< 0.02	< 0.02	< 0.02	< 0.02	< 0.02	0.02	< 0.02
Cd	0.02	0.02	< 0.01	0.02	0.02	< 0.01	0.02	0.06
Co	6.7	5.3	8.9	13.3	4.9	7	10	13.8
Cu	25.4	23.6	27.7	5	149	16	50	39.4
Hg	< 0.01	< 0.01	< 0.01	< 0.01	< 0.01	< 0.01	0.04	< 0.01
Mo	0.58	0.67	2.84	0.8	1.08	0.43	0.98	0.69
Ni	8.7	6.6	13.9	17.1	5.4	10.1	12.8	21.3
Pb	4.8	5.5	2.6	4.6	8.1	3.3	6.7	5
Sb	< 0.05	< 0.05	< 0.05	< 0.05	< 0.05	< 0.05	< 0.05	< 0.05
Se	< 1	< 1	< 1	< 1	< 1	< 1	1	< 1
Zn	54	45	62	41	37	56	73	94
Ce	272.3	121	141.4	224.2	311.6	201.6	434.9	304.7
Dy	5.71	4.17	5.34	5.88	4.52	6.76	6.24	5.73
Er	1.58	1.27	2.18	2.14	1.21	2.74	2.06	2.83
Eu	1.25	1.23	1.38	1.58	1.42	1.26	2.72	2.82
Gd	9.62	8.05	8.31	9.88	9.96	9.77	13.43	11.92
Ho	0.65	0.55	0.82	0.87	0.46	1.07	1.21	1.32
La	168.4	91.6	80.7	178.9	215.2	117.6	215.4	150.9
Lu	0.13	0.08	0.22	0.22	0.12	0.28	0.25	0.15
Nd	107	65.1	68.2	98.8	124.8	83.3	203.3	134.6
Pr	31.61	18.55	18.32	28.85	37.19	24.21	55.2	34.96
Sm	13.5	11.2	10.9	12.1	15	12.5	27.8	19
Tb	1.15	0.93	1.02	1.13	1.02	1.33	1.46	1.41
Tm	0.19	0.15	0.26	0.26	0.13	0.38	0.21	0.22
Yb	1.1	0.9	1.8	1.7	1	2.4	1.4	2.1

Table 4. Geochemical data from Rocinha Orthogneiss.

	Rocinha Orthogneiss										
SAMPLE	**RF-323**	**RF-323B**	**RF-323C**	**RF-466**	**RF-467**	**RF-311**	**FL-180***	**FL-181***	**FL-185***	**SF-182***	**RF-033**
Wt %											
SiO_2	74.33	70.37	72.94	68.54	71.19	77.38	75.56	75.99	77.47	75.5	72.39
TiO_2	0.3	0.29	0.15	0.29	0.31	0.17	0.14	0.2	0.27	0.13	0.2
Al_2O_3	13.4	13.06	11.82	13.43	13.19	12.15	11.8	11.83	12.5	11.12	11.06
Fe_2O_3	3.13	2.85	2.04	2.83	2.86	1.9	1.61	2.6	2.34	1.97	2.56
CaO	0.78	1.71	0.77	0.74	0.92	0.68	0.95	1.05	1.23	0.66	0.8
Cr_2O_3	< 0.01	< 0.01	< 0.01	< 0.01	< 0.01	< 0.01	< 0.01	< 0.01	< 0.01	< 0.01	< 0.01
K_2O	6.82	6.49	6.33	6.47	6.96	6.63	4.77	4.73	5.3	4.53	5.27
MgO	0.31	0.33	0.17	0.23	0.27	0.13	0.21	0.25	0.3	0.13	0.15
MnO	0.04	0.04	0.03	0.04	0.04	0.01	0.05	0.06	0.04	0.05	0.05
Na_2O	2.86	2.7	2.48	3.05	2.68	2.73	2.63	2.62	2.62	2.58	2.79
P_2O_5	< 0.01	< 0.01	0.12	< 0.01	< 0.01	< 0.01	0.03	0.09	0.08	0.03	0.04
Sum	0.19	0.29	0.41	0.23	0.16	0.23	0.17	0.08	0.23	0.52	0.04
LOI	102.12	98.11	97.25	95.72	98.57	101.98	97.91	99.51	102.39	97.21	95.34
ppm											
Ba	453	466	280	443	475	323	315	393	461	188	721
Be	4.6	3.6	3.2	6.3	3.8	3.8	5.3	5.5	3.9	3.8	4.5
Cs	10	9.37	4.88	10.87	6.95	3.66	16.76	17.18	9.06	7.02	4.6
Ga	20.5	20.4	19	22.1	20.4	19.6	21.1	22.2	21.8	23.4	18.6
Hf	9.63	10.04	5.05	10.5	10.27	7.73	14	21.92	21.92	18.66	7.07
Nb	26.91	23.47	18.64	27.63	22.56	21.01	24.35	25.88	22.57	23.7	25.52
Rb	298	286	285	297	285	314	365	339	267	338	227.2
Sn	7.1	9	6.4	11.4	7.8	11.4	7.4	8	4.5	8	4
Sr	50.2	120	59.2	50.9	52.7	79.4	70.5	90	77	35.8	79.9
Ta	4.79	4.13	2.79	4.02	2.86	2.79	4.12	3.66	3.06	3.78	1.67
Th	25	26.8	24.6	27.7	27.8	37.9	17.9	38.1	24.1	26.3	25.2
U	4.31	4.84	3.81	4.31	5.57	6.47	5.16	5.95	3.05	3.92	2.96
W	2.6	4.5	4.2	1.7	4.5	0.4	< 0.1	1.5	1.1	0.2	0.5
Y	54.22	60.06	54.35	71.24	57.22	60.77	46.1	46.34	41.83	68.2	51.03
Zr	338	329	164	367	379	240	95.6	156	190	120	243.3
Ag	< 0.01	< 0.01	0.04	0.02	0.03	0.06	0.16	0.15	0.08	0.12	< 0.01
Au	< 0.1	< 0.1	< 0.1	< 0.1	< 0.1	< 0.1	< 0.1	< 0.1	< 0.1	< 0.1	< 0.1
As	< 1	< 1	< 1	< 1	< 1	< 1	< 1	< 1	1	2	< 1
Bi	0.06	0.08	< 0.02	0.08	0.06	0.04	0.39	0.49	0.12	0.69	0.05
Cd	< 0.01	< 0.01	< 0.01	0.01	< 0.01	0.03	0.03	0.09	0.04	< 0.1	0.03
Co	2.3	2.2	1.2	2.9	2.3	0.8	1.6	2.4	2.7	1.4	1.5
Cu	2	2.5	2.5	16.8	6.9	5.3	6.7	9.2	6.7	5.2	3
Hg	< 0.01	< 0.01	< 0.01	< 0.01	< 0.01	< 0.01	< 0.01	< 0.01	0.02	< 0.01	0.02
Mo	0.23	0.25	0.53	2.31	0.98	1.24	0.32	0.69	0.39	0.31	0.65
Ni	1.7	2.1	2.2	5.6	2.1	1.4	2.2	2.9	3	2.2	1.4
Pb	5.9	7	7	7.3	5.7	4.8	2.5	4.3	23.4	5.8	3.3
Sb	< 0.05	< 0.05	< 0.05	0.22	0.07	< 0.05	0.07	0.08	< 0.05	0.07	< 0.05
Se	< 1	< 1	< 1	< 1	< 1	1	< 1	< 1	< 1	1	1
Zn	48	49	23	52	46	30	29	48	41	39	56
Ce	138.8	144.1	134.2	157.8	145.2	133.2	75.8	87.5	116	70.6	152.7
Dy	9.56	10.65	10.05	12.7	10.65	10.79	7.56	7.19	6.67	8.7	9.36
Er	5.52	5.81	5.45	7.32	6.07	6.07	4.11	4.35	3.59	5.11	6.01
Eu	1.3	1.22	0.77	1.38	1.18	0.57	0.68	0.78	1.1	0.68	1.36
Gd	9.73	11.56	10.09	13.63	11.37	10.76	7.89	6.35	8.73	9.38	9.82
Ho	1.97	2	1.86	2.47	2	2.03	1.46	1.47	1.33	1.74	2.08
La	85.7	95.7	85.8	106.1	92	92	43.4	45	63.8	37.8	70.2
Lu	0.88	0.83	0.69	1.03	0.76	0.8	0.64	0.69	0.54	0.75	0.83
Nd	54.7	61.4	56	71.8	62.5	59.1	36.6	34.2	51.9	38.9	63.3
Pr	16.2	17.66	16.33	20.23	17.8	17.17	10.33	9.83	14.32	10.06	16.86
Sm	10.4	11.2	10.5	13.7	11.6	11.4	7.8	6.9	9.3	8.4	11.8
Tb	1.72	1.73	1.6	2.12	1.78	1.76	1.19	1.01	1.22	1.47	1.79
Tm	0.97	0.93	0.81	1.11	0.88	0.88	0.63	0.61	0.5	0.75	0.71
Yb	5.6	5.5	5.2	7.2	5.5	5.8	3.8	4.6	3.3	5	5.1

zircon are homogeneous and these were analyzed with spots concentrated in the cores. The U-Pb analyses indicate a crystallization age of 2,734 ± 11 Ma (Fig. 6B).

Fulgêncio Orthogneiss

The investigated sample is a granitic gneiss (sample RF-243), as in Tab. 6. The BSE and CL images show abundant zircon crystals with concentric oscillatory zoning and thin (between 10 to 50 mm) overgrowths (Figs. 7A to 7C). The U-Pb results indicated an age of 1,996 ± 8 Ma (Fig. 7D). No significant differences were found between the ages of core and rims of zircons crystals analyses. Fulgêncio Orthogneiss has, therefore, a Paleoproterozoic granite protolith, which is slightly younger than others generated during Paleoproterozoic orogenesis within Borborema Province.

Table 5. Isotopic data from Entremontes Complex zircons (sample RF-179), *Universidade Federal do Rio Grande do Sul* data isotope laboratory.

RF-179	Ratios		Ages (Ma)												
Spot n°	%^{206}Pb	^{232}Th/^{238}U	^{207}Pb/^{206}Pb	1s(%)	^{207}Pb/^{235}U	1s(%)	^{206}Pb/^{238}U	1s(%)	^{207}Pb/^{206}Pb	1s(Ma)	^{207}Pb/^{235}U	1s(Ma)	^{206}Pb/^{238}U	1s(Ma)	Conc (%)
MT65_08_a	0.02	0.14	0.18852	0.7	13.8064	1.3	0.53116	1.0	2729	11	2737	12	2746	23	101
MT65_08_b	0.04	0.18	0.18564	0.7	12.2151	2.3	0.47723	2.2	2704	11	2621	21	2515	45	93
MT65_16_a	0.03	0.15	0.19160	0.7	13.4383	1.4	0.50869	1.2	2756	12	2711	13	2651	26	96
MT65_23	0.00	0.13	0.18717	0.8	13.0380	1.3	0.50522	1.0	2717	13	2682	12	2636	22	97
MT65_37	0.02	0.11	0.19039	0.7	14.9269	2.9	0.56863	2.8	2746	11	2811	27	2902	65	106
MT65_38	0.14	0.12	0.18644	1.0	13.3200	1.4	0.51816	1.0	2711	16	2703	13	2691	22	99
MT65_39	0.03	0.49	0.18257	0.9	10.9878	6.0	0.43649	5.9	2676	14	2522	56	2335	116	87
MT65_47	0.03	0.16	0.18769	0.6	13.1696	1.3	0.50889	1.1	2722	10	2692	12	2652	24	97
MT65_55	0.03	0.13	0.18890	0.8	11.9820	2.2	0.46004	2.1	2733	13	2603	21	2440	42	89

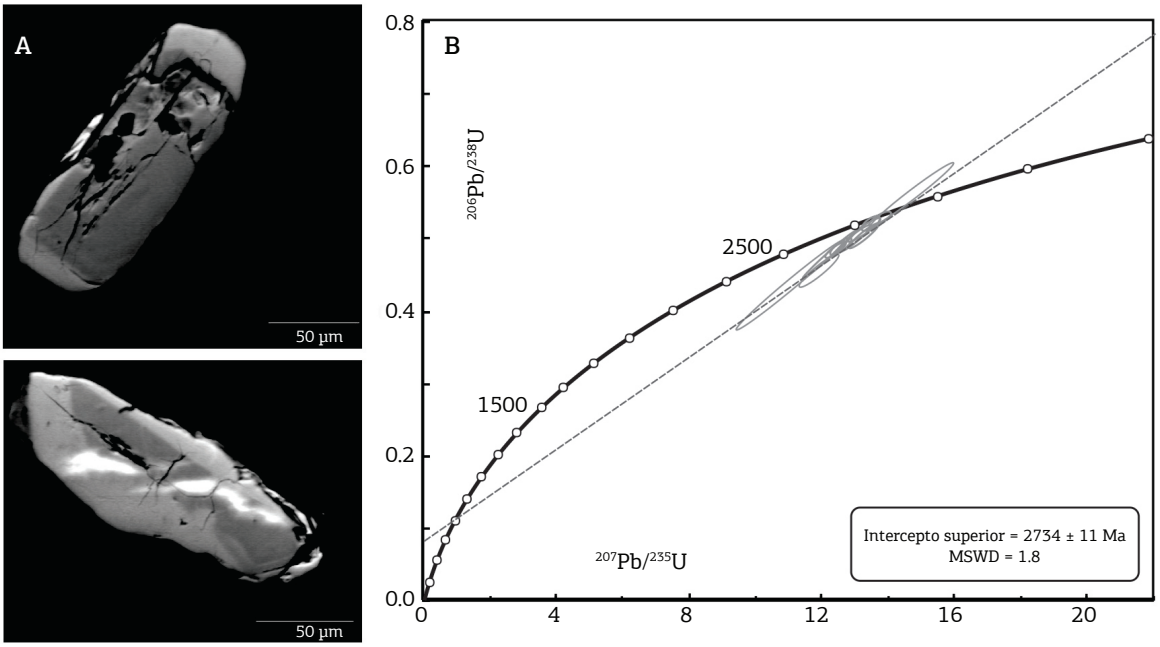

Figure 6. Geochronological data for zircon grains from the Entremontes Complex. (A) Backscattering images of zircon grains with sizes from small to medium, prismatic with rounded edges and a predominant proportion 3 x 1; (B) U-Pb zircon Concordia diagram.

Riacho Seco Gneissic-migmatitic Complex

Riacho Seco Gneissic-migmatitic Complex sample is a medium-grained equi-granular biotite granite-gneiss (sample RF-111). Zircons from this sample are rather heterogeneous in terms of shape and size, with elongated prismatic crystals, as well as rounded ones with concentric zoning. Overgrowths and corrosion features are therefore recognized (Figs. 8A to 8D). The U-Pb results are complex and difficult to interpret due to the variety of ages found for the different zircon populations (Tab. 7). Three major age groups are identified: 1,992 ± 27; 2,461 ± 24 and 2,704 ± 12 Ma (Figs. 9A to 9C), the first two discords show Neoproterozoic lower intercept ages (548 ± 76 Ma and 559 ± 40 Ma). In homogeneous crystals, Paleoproterozoic ages predominate, whereas in the heterogeneous crystals Archean ages are more seen with a few exceptions. Two zircon grains analyzed have differences in ages between core and rim, with Archean age in the core (2,526 to 2,711 Ga) and Paleoproterozoic age on the edge (2,003 to 2100 Ga). The age patterns of Riacho Seco Complex suggest that its igneous protoliths are the product of anatexis of Archean continental crust indicated by the abundant presence of inherited archean zircons.

Lobo Orthogneiss

Lobo Orthogneiss (Brito & Freitas 2011), recognized during Salgueiro mapping project, was dated by the U-Pb LA-ICPMS method on zircon at 994 ± 25 Ma (Brito & Marinho 2012). One additional sample of a granodiorite mylonite (sample RF-270) was dated (Tab. 8) and yielded a U-Pb zircon age of 974 ± 8 Ma

Table 6. Isotopic data from Fulgêncio Orthogneiss zircons (sample RF-243), UNB data isotope laboratory.

RF-243 Spot n°		Contents (ppm)		Ratios							Ages (Ma)						
	$\%^{206}Pb$	U	Th	$^{232}Th/^{238}U$	$^{207}Pb/^{206}Pb$	1s(%)	$^{207}Pb/^{235}U$	1s(%)	$^{206}Pb/^{238}U$	1s(%)	$^{207}Pb/^{206}Pb$	1s(Ma)	$^{207}Pb/^{235}U$	1s(Ma)	$^{206}Pb/^{238}U$	1s(Ma)	Conc (%)
006-Z03	0.00	105	45	0.43	0.12203	0.3	5.8279	0.6	0.34636	0.6	1986	6	1951	6	1917	9	97
010-Z05	0.01	93	35	0.38	0.12471	0.6	5.8422	1.1	0.33976	0.9	2025	10	1953	9	1886	15	93
011-Z06	0.51	259	76	0.29	0.12495	0.6	5.8089	0.8	0.33718	0.5	2028	10	1948	7	1873	9	92
012-Z07	0.00	105	45	0.43	0.12308	0.4	6.3994	0.8	0.37710	0.7	2001	7	2032	7	2063	12	103
013-Z08	0.02	148	32	0.21	0.12269	0.6	6.2300	0.9	0.36827	0.6	1996	11	2009	7	2021	10	101
014-Z09	0.00	93	35	0.38	0.12276	0.4	6.3961	0.7	0.37787	0.5	1997	7	2032	6	2066	9	103
019-Z11	0.00	148	32	0.21	0.12291	0.5	6.0520	0.7	0.35712	0.6	1999	8	1983	6	1968	10	98
020-Z12	0.01	93	35	0.38	0.12242	0.5	5.8440	1.0	0.34623	0.8	1992	8	1953	8	1917	14	96
021-Z13N	0.01	259	76	0.29	0.12252	0.4	6.1428	0.8	0.36362	0.7	1993	7	1996	7	1999	11	100
022-Z13B	0.01	105	45	0.43	0.12163	0.5	5.7957	0.8	0.34558	0.7	1980	10	1946	7	1913	11	97
023-Z14N	0.01	148	32	0.21	0.12256	0.8	6.0070	1.1	0.35549	0.7	1994	14	1977	10	1961	13	98
025-Z15	0.11	259	76	0.29	0.12137	0.5	5.8478	1.0	0.34945	0.9	1976	8	1954	9	1932	15	98
026-Z16B	0.00	105	45	0.43	0.12128	1.2	5.9997	1.4	0.35880	0.8	1975	21	1976	12	1976	13	100
031-Z17	0.00	93	35	0.38	0.12300	0.5	6.1247	0.9	0.36114	0.8	2000	9	1994	8	1988	14	99
032-Z18B	0.28	259	76	0.29	0.12156	0.5	5.4826	0.9	0.32710	0.7	1979	8	1898	8	1824	12	92
033-Z18N	0.01	105	45	0.43	0.11967	0.6	6.0576	1.3	0.36713	1.2	1951	11	1984	11	2016	20	103
035-Z20	0.07	93	35	0.38	0.11963	1.7	5.6153	1.9	0.34042	0.8	1951	30	1918	16	1889	13	97
036-Z21	0.19	259	76	0.29	0.12006	0.4	5.6883	0.9	0.34361	0.8	1957	8	1930	8	1904	13	97
040-Z22N	0.02	148	32	0.21	0.12223	0.7	6.1913	1.2	0.36739	1.0	1989	12	2003	10	2017	17	101
041-Z23B	0.22	93	35	0.38	0.12395	0.9	6.0320	1.5	0.35294	1.2	2014	16	1980	13	1949	21	97
042-Z23N	0.23	259	76	0.29	0.12146	0.5	5.5772	1.0	0.33302	0.8	1978	10	1913	8	1853	13	94
043-Z24	0.01	105	45	0.43	0.12021	0.5	5.9925	1.0	0.36154	0.8	1959	10	1975	8	1989	14	102
045-Z26	0.00	93	35	0.38	0.12319	0.4	6.1753	0.8	0.36356	0.7	2003	7	2001	7	1999	12	100
046-Z27	0.00	259	76	0.29	0.12264	0.3	6.0005	0.7	0.35485	0.6	1995	6	1976	6	1958	9	98
049-Z28B	0.01	105	45	0.43	0.12248	0.3	5.9105	0.7	0.34999	0.6	1993	6	1963	6	1935	10	97
051-Z29B	0.00	93	35	0.38	0.11917	0.4	5.3140	0.8	0.32342	0.7	1944	8	1871	7	1806	10	93
052-Z29N	0.01	259	76	0.29	0.11805	0.4	4.8465	1.2	0.29774	1.2	1927	8	1793	10	1680	17	87
053-Z30B	0.18	105	45	0.43	0.12271	0.5	5.9061	0.9	0.34907	0.7	1996	9	1962	8	1930	12	97
054-Z30N	0.06	148	32	0.21	0.12388	0.8	5.8866	1.1	0.34465	0.7	2013	15	1959	10	1909	12	95
053-Z30B	0.18	259	76	0.29	0.12271	0.5	5.9061	0.9	0.34907	0.7	1996	9	1962	8	1930	12	97
054-Z30N	0.06	105	45	0.43	0.12388	0.5	5.8866	0.9	0.34465	0.7	2013	8	1959	8	1909	12	95
055-Z31	0.00	148	32	0.21	0.12295	0.6	6.0402	0.9	0.35631	0.6	1999	11	1982	8	1965	11	98

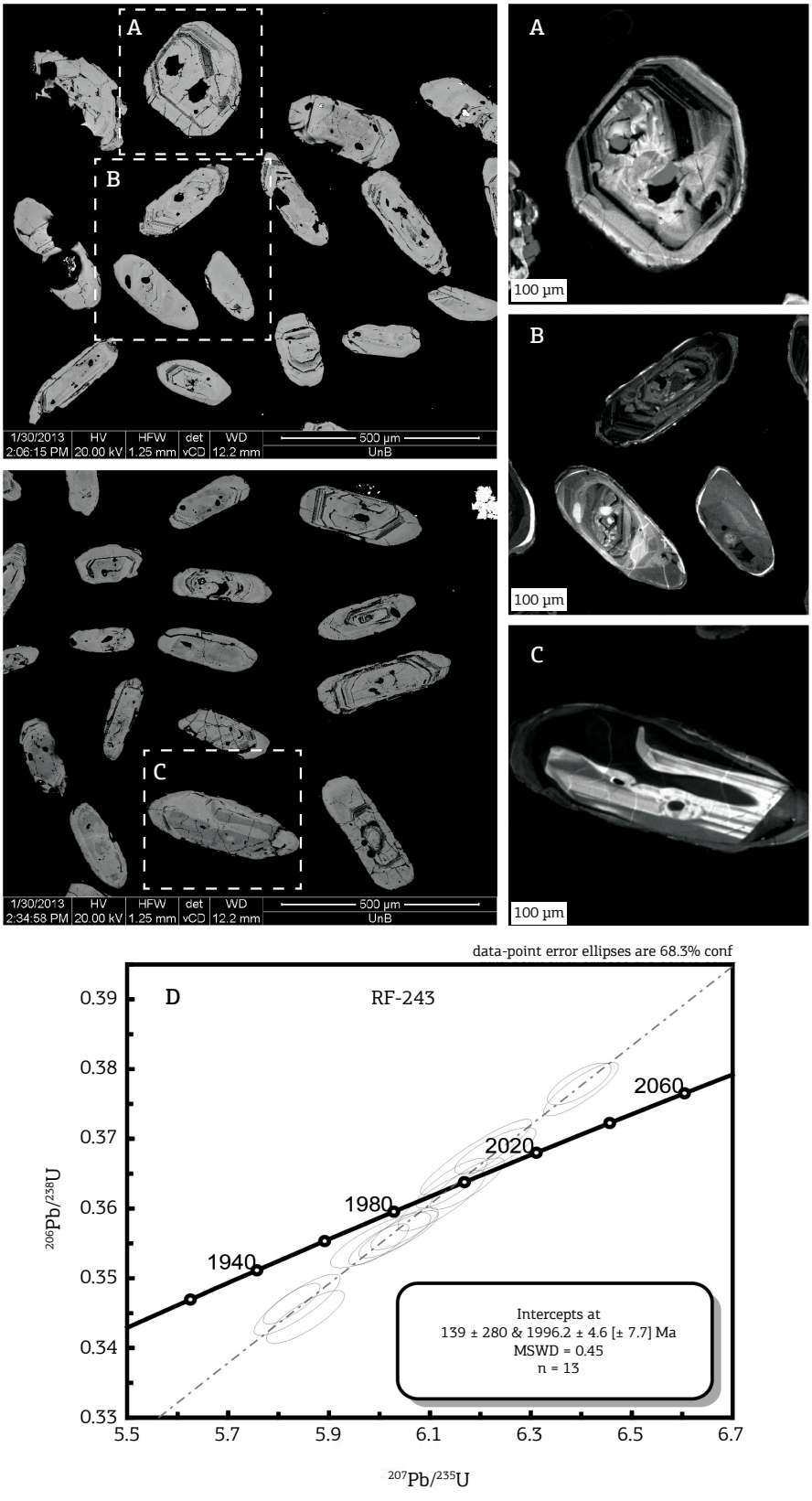

Figure 7. Results of zircons analyzes from Fulgêncio Orthogneiss. Backscatter electron images left with details of crystals imaged by cathodoluminescence at right. (A) Image of zircon with metamictic core and rim zoned; (B) Crystals showing oscillatory zoning besides crystal homogeneous; (C) Prismatic crystal with irregular nucleus; (D) Concordia diagram highlighting the Orosirian age unit.

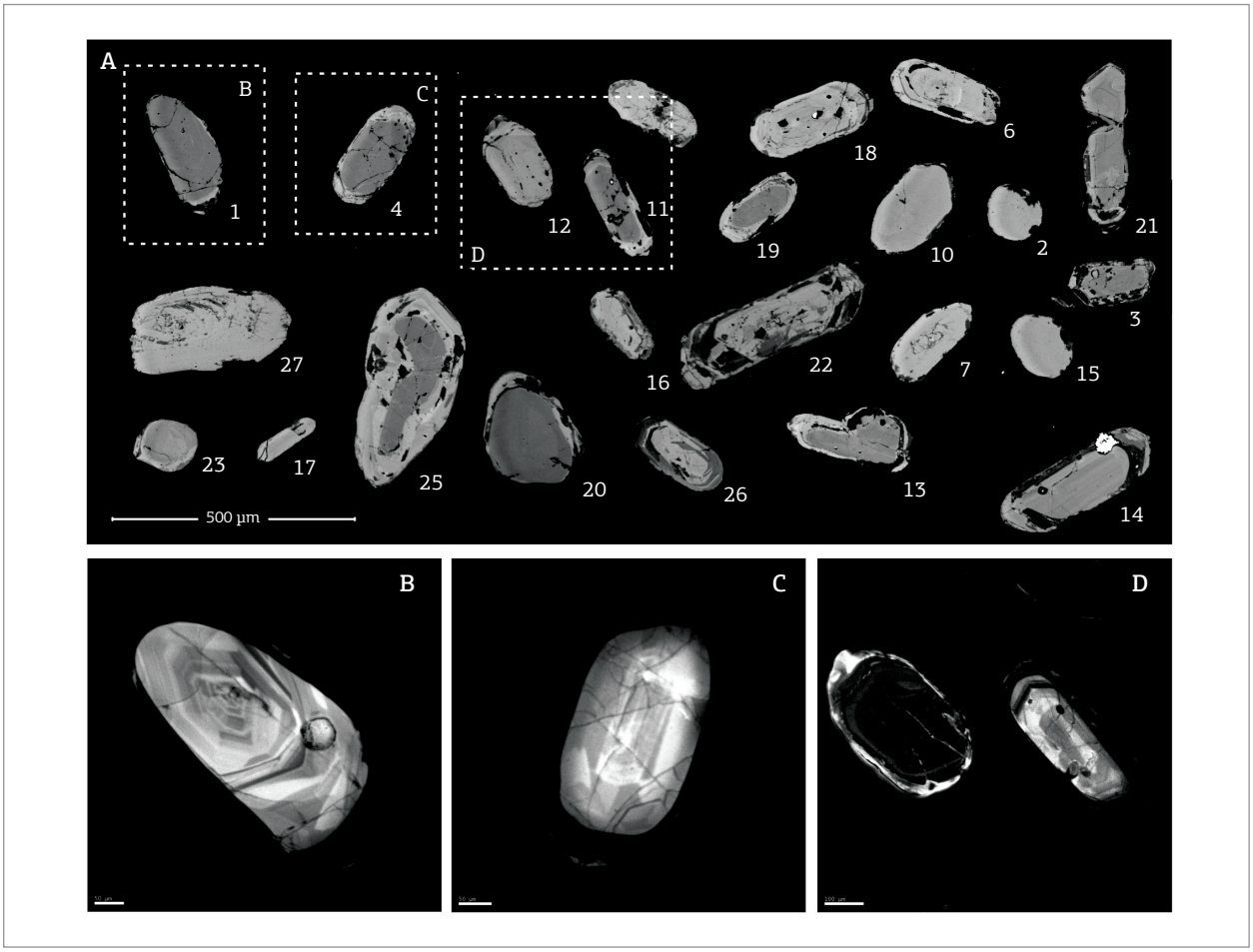

Figure 8. Zircons microscope images from granitic orthogneiss sample (RF-111), Riacho Seco Gneissic-migmatitic Complex. (A) Backscatter images of some zircons grains from Riacho Seco Complex sample (RF-111); (B to D) Cathodoluminescence images showing different features on zircon grains, with elongated prismatic crystals, others rounded and showing concentric zoning, overgrowths and corrosion features are recognized in some grains.

Table 7. Isotopic data from Riacho Seco Gnaissic-migmatitic Complex (sample RF-111), UNB data isotope laboratory.

RF-111 Spot n°		Contents (ppm)		Ratios							Ages (Ma)						
	%^{206}Pb	U	Th	^{232}Th/^{238}U	^{207}Pb/^{206}Pb	1s(%)	^{207}Pb/^{235}U	1s(%)	^{206}Pb/^{238}U	1s(%)	^{207}Pb/^{206}Pb	1s(Ma)	^{207}Pb/^{235}U	1s(Ma)	^{206}Pb/^{238}U	1s(Ma)	Conc (%)
004-Z01	0.01	93	35	0.38	0.18568	0.6	13.2410	0.9	0.51721	0.8	2704	9	2697	9	2687	17	99
005-Z02	0.50	259	76	0.29	0.08956	2.1	2.1598	2.4	0.17489	1.1	1416	40	1168	16	1039	10	73
006-Z03	0.73	105	45	0.43	0.16841	0.6	9.2062	1.8	0.39648	1.7	2542	10	2359	17	2153	32	85
007-Z04	0.04	148	32	0.21	0.18232	2.0	7.4191	3.1	0.29513	2.4	2674	32	2163	28	1667	36	62
008-Z05	0.21	93	35	0.38	0.12053	0.4	5.8244	1.0	0.35048	0.9	1964	8	1950	9	1937	15	99
010-Z07	0.17	105	45	0.43	0.10822	0.8	3.1963	1.7	0.21421	1.5	1770	15	1456	13	1251	17	71
013-Z08	0.20	148	32	0.21	0.11741	0.6	4.4552	1.8	0.27522	1.7	1917	10	1723	15	1567	24	82
014-Z09	0.04	93	35	0.38	0.11099	0.5	3.8159	1.2	0.24935	1.1	1816	9	1596	10	1435	14	79
015-Z10	0.00	259	76	0.29	0.12293	0.6	6.4063	1.1	0.37795	0.9	1999	11	2033	9	2067	15	103
016-Z11	0.35	105	45	0.43	0.18141	0.5	10.6838	1.5	0.42714	1.4	2666	8	2496	14	2293	28	86
017-Z12	0.01	148	32	0.21	0.15743	0.7	9.0012	0.9	0.41467	0.6	2428	12	2338	8	2236	11	92
018-Z13N	0.13	93	35	0.38	0.16683	1.4	8.9837	1.9	0.39056	1.3	2526	23	2336	17	2125	24	84
019-Z13B	0.07	259	76	0.29	0.13013	0.7	3.7196	1.3	0.20731	1.1	2100	13	1576	10	1214	12	58
020-Z14	0.20	105	45	0.43	0.17081	0.8	10.7499	2.4	0.45646	2.3	2566	13	2502	22	2424	46	94
026-Z16	0.16	259	76	0.29	0.11277	0.8	4.1028	1.9	0.26386	1.7	1845	14	1655	15	1510	23	82
027-Z17	0.11	105	45	0.43	0.16034	0.9	7.4905	2.9	0.33882	2.8	2459	15	2172	26	1881	45	76
028-Z18	0.00	148	32	0.21	0.16050	1.9	10.4418	2.3	0.47185	1.2	2461	33	2475	21	2492	25	101
030-Z19N	0.01	259	76	0.29	0.18641	1.4	12.6794	1.8	0.49333	1.2	2711	22	2656	17	2585	26	95
029-Z19B	0.06	93	35	0.38	0.12319	1.6	3.3622	3.3	0.19794	2.9	2003	28	1496	25	1164	31	58
034-Z20	0.00	148	32	0.21	0.18511	0.5	12.8634	0.8	0.50398	0.6	2699	9	2670	8	2631	13	97
035-Z21	0.24	93	35	0.38	0.18400	0.7	10.5409	1.7	0.41548	1.6	2689	11	2484	16	2240	30	83

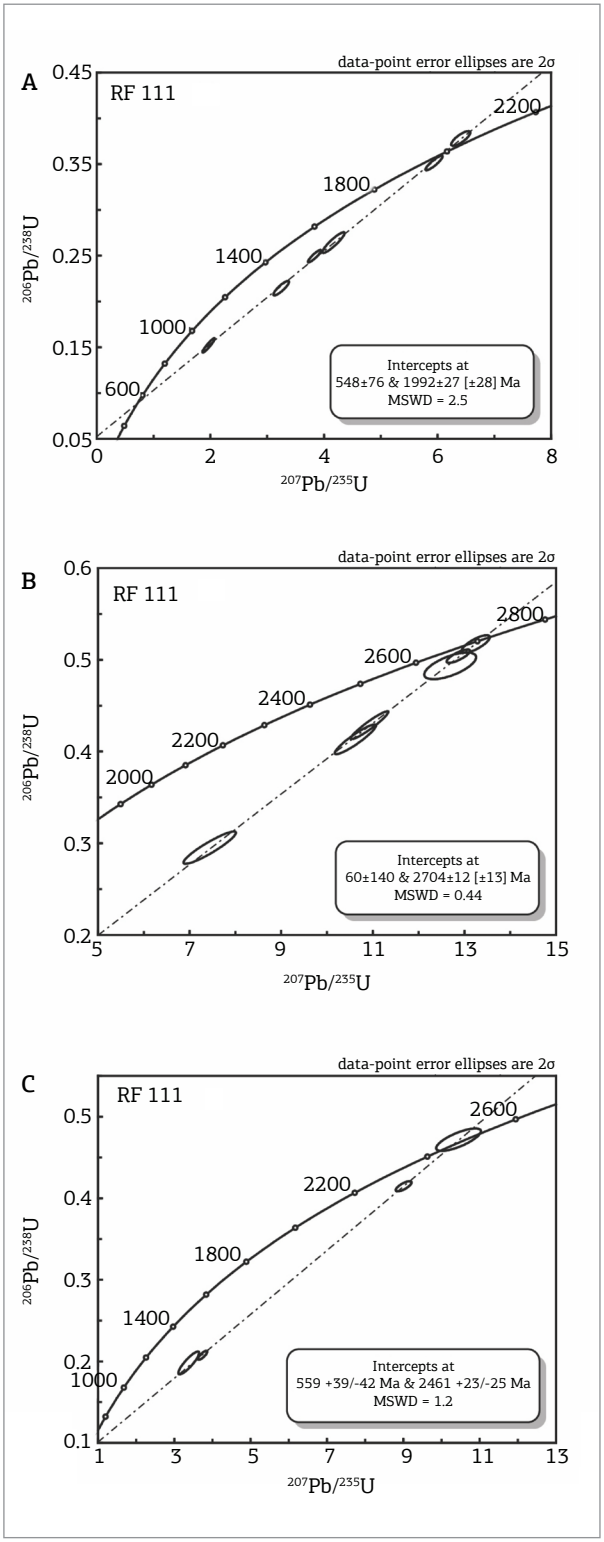

Figure 9. Concordia diagrams for zircon grains from granitic orthogneiss sample RF-111, showing tree different age groups. (A) Concord diagram with majority of zircon grains being of Paleoproterozoic (Orosirian) age; (B) Concordia diagram for the second zircon population with Neoarchean age; (C) Concordia diagram for small-zircon populations that yielded Siderian (Paleoproterozoic) ages.

(Fig. 10B) interpreted as the crystallization age of the protolith. Zircons showing Stenian periods are also observed in this sample. The crystals are predominantly prismatic; some grains show homogenous texture and narrow zoned edges and others show oscillatory concentric zoning, no significant differences ages were found between spots on core and rim (Fig. 10A). Data indicate that the granite/granodiorite protolith of Lobo Orthogneiss crystallized during the Cariris Velhos Event and probably suffered shear deformation during the Brasiliano Orogeny.

Rocinha Orthogneiss

Sample RF-323 of Rocinha Orthogneiss (Cruz & Accioly 2013) was investigated. The zircon grains are prismatic, with rounded edges and aspect ratios ranging from 2:1 to 4:1. The elongated grains have reddish color and some inclusions, whereas the smaller ones tend to be pink. The BSE images show predominance of homogeneous grains, although some thin overgrowths are observed (Fig. 11A). Some crystals showing cores and wider "porous" rims may suggest an alteration process (Figs. 9C to 9D). One sample collected from the type locality of Rocinha Orthogneiss is dated (RF-323) (Tab. 9), and the analyses indicate a concordia age of 956 ± 2 Ma (Fig. 11B).

Nd Isotopes

Sm-Nd analyses were carried out on 23 whole-rock samples (Tab. 10, Fig. 12). Considering the Nd isotopic results, combined with field observations, geochemical and geochronological data, six main groups of granitoids are identified:

- Neoproterozoic intrusions or Brasiliano granitoids (Ediacaran-Criogenian) comprising Bendó Orthogneiss (sample RF-415, model age of 1.79 Ga and e_{Nd} – 600 Ma – of -9.97), Ibó Migmatites with medium grained biotite-amphibole migmatite including metasedimentary xenoliths (sample RF-022, model age of 1.43 Ga and e_{Nd} – 600 Ma – of -4.23), and grey granitic migmatite with muscovite and biotite and metasedimentary xenoliths (sample RF-068, model age of 1.88 Ga and e_{Nd} – 600 Ma – of -6.09), Chorrochó Augen-gneiss (sample RF-027, model age of 1.25 Ga and e_{Nd} – 600 Ma – of -2.80), and fine grained biotite-amphibole orthogneiss (sample RF-322, model age of 1.54 Ga and e_{Nd} – 600 Ma – of -4.16).
- Cariris Velhos granites (Tonian-Estenian), which comprise granitic migmatite (sample RF-003, model age of 1.37 Ga and e_{Nd} – 1 Ga – of +0.64), the

coarse grained granite gneiss of Rocinha Orthogneiss (sample RF-010, model age of 1.46 Ga and e_{Nd} – 1 Ga – of +0.63, sample RF-033, model age of 1.56 and e_{Nd} (1 Ga) of -1.29, sample RF-323, model age of 1,45 and e_{Nd} (1 Ga) of -0.32). The granodioritic mylonitic gneiss from Lobo Orthogneiss (sample RF-270, model age of 1.54 Ga and e_{Nd} (1 Ga) of -1.23).

- Paleoproterozoic granites of PEAL, which corresponds to Fulgêncio Orthogneiss. Three different facies were investigated: augen-gneiss (sample RF-243, model age of 2.55 Ga and e_{Nd} (2 Ga) of -5.55), fine grained granitic gneiss (sample RF-244, model age of 2.79 Ga and e_{Nd} (2 Ga) of -10.06), and coarse grained granitic migmatite (sample RF-267, model age of 2.49 Ga and e_{Nd} (2 Ga) of -5.52; sample RF-040, model age of 2.68 and e_{Nd} (2 Ga) of -6.80; sample RF-165, model age of 2.60 Ga and e_{Nd} (2 Ga) of -6.18).
- Paleoproterozoic granitoids from RSN, comprising metamorphosed granites and amphibolites from Riacho Seco Gneissic-migmatitic Complex, represented by: medium grained equigranular granite gneiss (sample RF-111, model age of 3.14 Ga and e_{Nd} (2 Ga) of -13.30) and coarse grained granite gneiss (sample RF-136, model age of 3.14 and e_{Nd} (2 Ga) of -14.02). Other units recognized in the RSN are the Caraíbas Migmatite with two samples of granitic

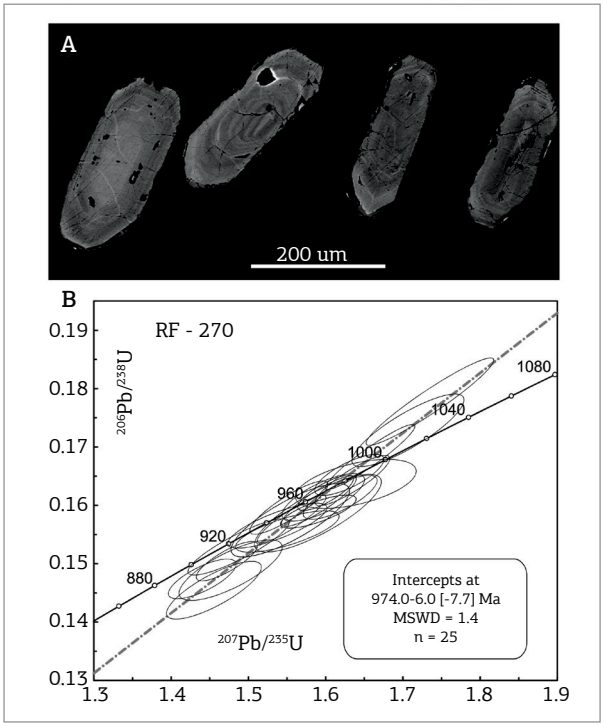

Figure 10. U-Pb data from sample RF-270 for the Lobo Orthogneiss. (A) Backscatter images for some of the analyzed zircon grains, some grains show homogenous texture and narrow zoned edges, and others present oscillatory concentric zoning, no significant differences in age were found between spots on core and rim; (B) U-Pb zircon age Concordia diagram.

Table 8. Isotopic data from Lobo Orthogneiss zircons (sample RF-270), UNB data isotope laboratory.

RF-270 Spot n°		Contents (ppm)		Ratios							Ages (Ma)						
	$\%^{206}Pb$	U	Th	$^{232}Th/^{238}U$	$^{207}Pb/^{206}Pb$	1s(%)	$^{207}Pb/^{235}U$	1s(%)	$^{206}Pb/^{238}U$	1s(%)	$^{207}Pb/^{206}Pb$	1s(Ma)	$^{207}Pb/^{235}U$	1s(Ma)	$^{206}Pb/^{238}U$	1s(Ma)	Conc (%)
006-Z03	0.02	105	45	0.43	0.07181	0.6	1.5913	1.2	0.16072	1.1	980	12	967	8	961	10	98
008-Z05	0.01	93	35	0.38	0.07159	0.5	1.5560	1.2	0.15764	1.1	974	10	953	7	944	9	97
009-Z06	0.04	259	76	0.29	0.07099	0.6	1.4723	1.1	0.15043	0.9	957	13	919	7	903	8	94
014-Z09	0.02	93	35	0.38	0.07277	0.7	1.6189	1.2	0.16136	1.0	1007	15	978	8	964	9	96
015-Z10	0.01	259	76	0.29	0.07158	0.7	1.6306	1.1	0.16521	0.9	974	14	982	7	986	8	101
018-Z12B	0.02	93	35	0.38	0.07160	1.2	1.5543	2.0	0.15744	1.6	975	24	952	12	943	14	97
020-Z14	0.01	105	45	0.43	0.07157	0.5	1.5999	0.9	0.16212	0.8	974	11	970	6	969	7	99
023-Z15	0.02	148	32	0.21	0.07258	1.0	1.5905	1.3	0.15893	0.7	1002	21	966	8	951	6	95
018-Z12B	0.02	93	35	0.38	0.07160	1.2	1.5543	2.0	0.15744	1.6	975	24	952	12	943	14	97
020-Z14	0.01	105	45	0.43	0.07157	0.5	1.5999	0.9	0.16212	0.8	974	11	970	6	969	7	99
023-Z15	0.02	148	32	0.21	0.07258	1.0	1.5905	1.3	0.15893	0.7	1002	21	966	8	951	6	95
028-Z20	0.02	93	35	0.38	0.07054	0.6	1.5524	1.3	0.15961	1.2	944	13	951	8	955	10	101
029-Z21	0.05	259	76	0.29	0.07088	0.8	1.4404	1.2	0.14739	0.9	954	17	906	7	886	8	93
030-Z22	0.01	105	45	0.43	0.07144	0.5	1.6575	1.4	0.16828	1.4	970	9	992	9	1003	13	103
037-Z26	0.04	148	32	0.21	0.07124	1.4	1.5375	1.7	0.15652	1.0	964	28	945	10	937	9	97
039-Z28	0.04	259	76	0.29	0.07263	1.6	1.6390	2.0	0.16367	1.0	1004	33	985	12	977	9	97
043-Z30	0.03	148	32	0.21	0.07056	1.3	1.4873	1.8	0.15288	1.3	945	26	925	11	917	11	97
044-Z31	0.03	93	35	0.38	0.07177	0.9	1.5968	1.4	0.16137	1.0	979	18	969	9	964	9	98
052-Z36	0.01	105	45	0.43	0.07218	0.6	1.6347	1.2	0.16425	1.1	991	11	984	8	980	10	99
054-Z38	0.04	93	35	0.38	0.07195	1.2	1.4771	1.8	0.14889	1.4	985	24	921	11	895	12	91
055-Z39	0.03	259	76	0.29	0.07258	1.0	1.4555	1.7	0.14545	1.4	1002	21	912	10	875	11	87
057-Z41	0.01	148	32	0.21	0.07079	0.9	1.7350	1.9	0.17776	1.7	951	19	1022	13	1055	17	111
059-Z43	0.03	259	76	0.29	0.07269	1.2	1.5900	2.1	0.15864	1.7	1005	25	966	13	949	15	94
064-Z45n	0.02	148	32	0.21	0.07231	1.5	1.5505	1.8	0.15552	0.9	995	30	951	11	932	8	94
084-Z61	0.02	93	35	0.38	0.07160	0.9	1.7065	1.7	0.17286	1.5	975	19	1011	11	1028	14	105

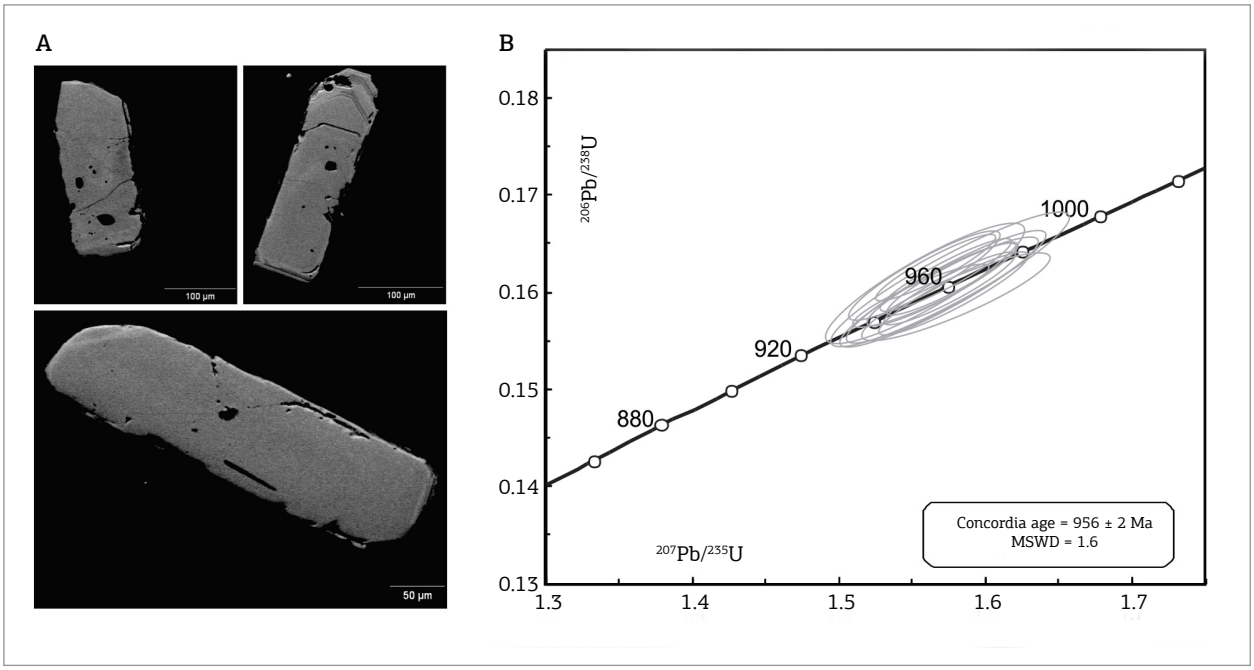

Figure 11. Geochronological data analysis sample of Rocinha Orthogneiss. (A) Backscatter electron images illustrating the predominant characteristics of the analyzed zircons, prismatic and homogeneous crystals, with the presence of narrow zoned edges; (B) Concordia diagram for zircon from the Rocinha Orthogneiss sample.

Table 9. Isotopic data from Rocinha Orthogneiss zircons (sample RF-323), *Universidade Federal do Rio Grande do Sul* data isotope laboratory.

RF-323 Spot n°		Ratios						Ages (Ma)							
	%^{206}Pb	^{232}Th/^{238}U	^{207}Pb/^{206}Pb	1s(%)	^{207}Pb/^{235}U	1s(%)	^{206}Pb/^{238}U	1s (%)	^{207}Pb/^{206}Pb	1s(Ma)	^{207}Pb/^{235}U	1s(Ma)	^{206}Pb/^{238}U	1s(Ma)	Conc (%)
MT32_01	0.06	0.21	0.07109	0.7	1.54777	1.2	0.15791	0.9	960	15	950	7	945	8	98
MT32_08	0.04	0.16	0.07113	0.7	1.60268	1.4	0.16343	1.2	961	14	971	9	976	11	102
MT32_10	0.06	0.21	0.07004	0.7	1.55387	1.3	0.16089	1.0	930	15	952	8	962	9	103
MT32_20	0.04	0.23	0.07059	0.6	1.56495	1.2	0.16078	1.1	946	11	956	8	961	10	102
MT32_21	0.03	0.27	0.07073	0.5	1.53479	1.0	0.15738	0.8	950	11	944	6	942	7	99
MT32_23	0.06	0.21	0.07124	0.7	1.58430	1.4	0.16130	1.3	964	14	964	9	964	11	100
MT32_27	0.02	0.24	0.07061	0.6	1.53077	1.0	0.15724	0.8	946	12	943	6	941	7	100
MT32_29	0.08	0.21	0.07029	0.8	1.57387	1.4	0.16239	1.1	937	16	960	8	970	10	104
MT32_31	0.09	0.26	0.07011	0.8	1.56719	1.1	0.16213	0.8	932	16	957	7	969	8	104
MT32_38	0.06	0.17	0.07107	0.9	1.57600	1.3	0.16084	0.9	959	19	961	8	961	8	100
MT32_39	0.05	0.27	0.07137	0.6	1.58020	1.4	0.16058	1.3	968	12	962	9	960	11	99
MT32_38	0.00	0.16	0.07172	1.1	1.58902	1.4	0.16070	0.9	978	22	966	9	961	8	98
MT32_43	0.09	0.19	0.07026	0.8	1.57160	1.2	0.16223	0.9	936	16	959	8	969	8	104
MT32_46	0.21	0.22	0.07053	1.0	1.55485	1.7	0.15988	1.4	944	20	952	10	956	12	101

migmatite (sample RF-128, model age of 2.75 and e_{Nd} (2 Ga) of -9.59; sample RF-249, model age of 2.61 Ga and e_{Nd} (2 Ga) of -1.97).

- Archean granites from PEAL represented by amphibole orthogneisses of the Entremontes Complex (sample RF-179, model age of 3.17 Ga and e_{Nd} (2.7 Ga) of -3.76).
- Granites within São Francisco Craton comprising pinkish alkali-rich migmatite near Riacho Seco, Curaça, Bahia State (sample RF-261, model age of 3.59 and e_{Nd} (2.7 Ga) of -6.70), and mafic biotite gneiss with garnet and sillimanite found near Santa Maria da Boa Vista, Pernambuco State (sample RF-171, model age of 2.7 Ga and e_{Nd} (2 Ga) of -1.61).

Table 10. Isotopic data from Sm-Nd of the study rocks.

Sample	Sm(ppm)	Nd(ppm)	$^{147}Sm/^{144}Nd$	$^{143}Nd/^{144}Nd \pm 2SE$	e_{Nd} (0)	e_{Nd} (600 Ma)	(Ga)
RF 022	4.429	23.747	0.1127	0.512091 ± 13	-10.68	-4.23	1.43
RF 027	10.143	60.474	0.1014	0.51212 ± 32	-10.11	-2.80	1.25
RF 068	0.619	2.731	0.1371	0.512092 ± 9	-10.66	-6.09	1.88
RF 322	15.443	74.099	0.1260	0.5121470 ± 25	-9.58	-4.16	1.54
RF 415	4.551	25.801	0.1066	0.5117733 ± 13	-16.87	-9.97	1.79
						e_{Nd} (1 Ga)	
RF 003	6.466	36.024	0.1085	0.512092 ± 17	-10.64	0.64	1.37
RF 010	10.845	50.698	0.1293	0.512228 ± 13	-8.00	0.63	1.46
RF 033	12.198	62.360	0.1182	0.512057 ± 13	-11.33	-1.29	1.56
RF 270	5.278	27.755	0.1150	0.512039 ± 11	-11.68	-1.23	1.54
RF 323	12.094	64.891	0.1127	0.5120705 ± 15	-11.07	-0.32	1.45
						e_{Nd} (2 Ga)	
RF 040	11.781	75.738	0.0940	0.510939 ± 13	-33.14	-6.18	2.68
RF 111	5.326	33.181	0.0970	0.510647 ± 13	-38.83	-13.30	3.14
RF 128	1.865	14.620	0.0771	0.510574 ± 15	-40.27	-9.59	2.75
RF 136	9.559	62.650	0.0922	0.510547 ± 9	-40.79	-14.02	3.14
RF 165	13.048	89.247	0.0884	0.510897 ± 17	-33.97	-6.18	2.6
RF 171	3.589	22.049	0.0984	0.511001 ± 19	-31.94	-6.72	2.7
RF 243	8.227	58.814	0.0846	0.510879 ± 3	-34.31	-5.55	2.55
RF 244	24.318	185.700	0.0792	0.510578 ± 2	-40.18	-10.06	2.79
RF 249	4.173	17.774	0.1419	0.511816 ± 10	-16.03	-1.97	2.61
RF 267	23.038	202.566	0.0687	0.510671 ± 3	-38.37	-5.52	2.49
						e_{Nd} (2.7 Ga)	
RF 179	14.362	83.267	0.1043	0.5107796 ± 16		-3.76	3.17
RF 261	24	103.108	0.1313	0.511132 ± 9	-29.38	-6.70	3.59

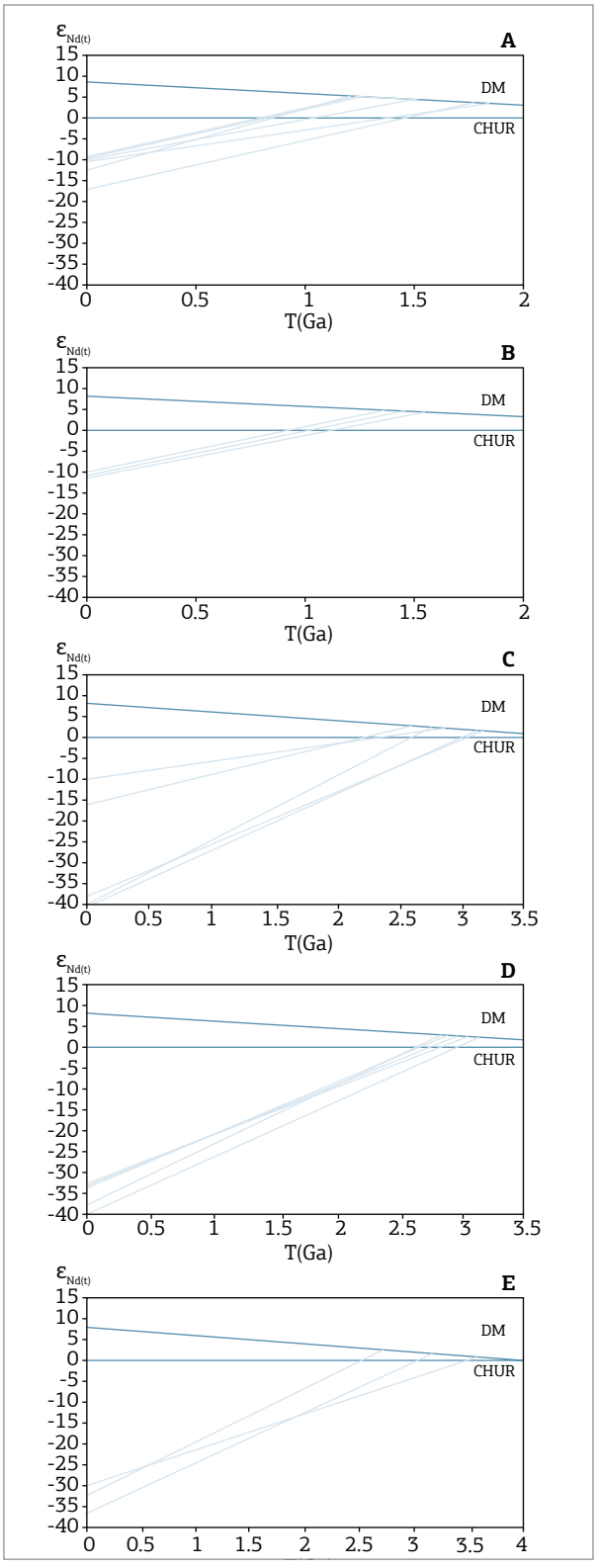

Figure 12. Diagram evolution of Nd to study rocks: (A) e_{Nd} from Brazilian rocks from Pernambuco-Alagoas Domain (PEAL); (B) e_{Nd} Cariris Velhos rocks from PEAL; (C) e_{Nd} Paleoproterozoic rocks from PEAL; (D) e_{Nd} Paleoproterozoic rocks from Riacho Seco Nucleus; (E) e_{Nd} São Francisco Craton rocks and Entremontes Complex.

DISCUSSION

The Entremontes Complex and metaplutonic bodies from RSN show Archean U-Pb and Sm-Nd ages, similar to rock units identified in the Congo and São Francisco Cratons (Bizzi *et al.* 2003; Teixeira *et al.* 2010), implying a correlation with the cratonic rocks.

Such Complex presents U-Pb zircon age of 2,734 ± 11 Ma and Sm-Nd model age of 3.16 Ga and e_{Nd} (T) of -3.8. These data imply anatexis of, or contamination with, older continental crust in the granitoid protholith genesis. The Entremontes Complex may be considered an allochthonous strip or basement inlier within the Western PEAL (Cruz 2013). One possibility to be considered is that it would be a fragment of the São Francisco Craton strongly deformed and displaced by the Brasiliano tectonics. An alternative hypothesis is that it may represent a microplate accreted to the Northern margin of São Francisco Craton during the Brasiliano orogeny.

The geochemical data reveal characteristics that are typically associated with intra-plate magmatism; however, others are common in subduction related granitoids. The Entremontes Complex, as indicated by the chemical data, is related to A-type magmatism most likely in a post-collisional setting during the end of Archean. Other units, in Borborema Province and São Francisco Craton, show similar ages and characteristics (Dantas *et al.* 2004; Teixeira 1997). The Entremontes Complex is the oldest rock unit in the PEAL.

The crystalline basement of the RSN represented by Riacho Seco Gneissic-migmatitic Complex presents a complex evolution, with Archean (2,704 ± 12 Ma) and Paleoproterozoic (1,992 ± 27 and 2,461 ± 24) zircons, besides lower intercept ages (548 ± 76 Ma and 559 ± 40 Ma). Despite the array of zircon populations, the petrographic evidence clearly points to an igneous origin of these rocks. The Th-U ratios and images of zircon grains were not conclusive to separate the different zircon population ages in igneous or metamorphic. The age pattern suggests that igneous protoliths crystallized in the Paleoproterozoic are the result of reworking of Archean crust, with the unit also suffering the effects of the Brasiliano cycle. Other hypothesis would be the RSN rocks are Archean and metamorphosed with partial melting during the Paleoproterozoic. Two additional localities in the Riacho Seco gneissic-migmatitic Complex had samples analyzed (Brito Neves, personal communication). Additional data confirm the complexity of geological processes, which those rocks had gone through.

Both samples presented three main age groups: 3.4, 2.65, and 2.0 Ga; 3.2, 2.55, and 2.1 Ga. The RSN is located close to the boundary between the craton and PEAL, and it is difficult to establish which of the two tectonic domains it belongs to. Due the complexity showed by the data acquired, further studies are needed to better define this unit.

Most Paleoproterozoic rocks in Borborema Province have ages between 2.3 and 2.0 Ga (Brito Neves *et al.* 2000; Neves 2003; Van Schmus *et al.* 2008). Fulgêncio Orthogneiss, however, has the age of 1.9 Ga, indicating a later stage in the Paleoproterozoic orogeny, a notion that is reinforced by their chemical characteristics associated with post-collisional setting. Few basement areas found in the Borborema Province have similar ages (Neves *et al.* 2014).

The U-Pb analyzes of zircon in Rocinha Orthogneiss indicate a concordia age of 956 ± 2 Ma, slightly younger compared with the average age of Cariris Velhos granite known in literature (990 – 960 Ma), including Lobo Orthogneiss (Brito & Marinho 2012). The Sm-Nd isotopic data yielded a model age value of 1.4 Ga and $e_{Nd}(T)$ of -0.8, which represents contamination with, or anatexis of, older crustal material (Cruz & Accioly 2013).

The large volume of Cariris Velhos granites (Tonian-Stenian) is remarkable. Its counterparts in Africa are still unknown, however these rocks are abundant in the Alto Pajeú Domain of the Central Sub-province further to the North (Santos *et al.* 2010; Guimarães *et al.* 2012), and therefore Cariris Velhos Belt is extended to the Western PEAL. A variety of granitic intrusions attributed to the Cariris Velhos Event has chemical characteristics similar to volcanic arc granites as well as to A-type post-collisional granites (Cruz & Accioly 2013; Santos *et al.* 2010; Kozuch 2003), suggesting that the Cariris Velhos event involved subduction process and does not represent purely an extensional episode.

Brasiliano plutons with Mesoproterozoic model ages are exposed in the Eastern PEAL, such as Águas Belas Pluton (Silva Filho *et al.* 2010). These bodies may be correlated with Brasiliano plutons in the Western part of the domain (Tab. 8).

The granitic-gneissic rocks in the Western PEAL with ages ranging from 1.0 to 0.6 Ga (Brasiliano and Cariris Velhos plutons) show TDM periods between 1.2 and 1.8 Ga. These model ages are quite similar to those found in the Central African Fold Belt, in which TDM ages range from 1.0 to 1.8 Ga, mainly in the Adamawa-Yade Domain (Van Schmus *et al.* 2008).

CONCLUSIONS

Based on U-Pb and Sm-Nd isotopic data gathered in this study, it was possible to divide the granitoids of the study area (covering approximately 70% of the area of the Western Pernambuco-Alagoas Domain) into six main groups:

- Brasiliano granites (Cryogenian-Ediacaran), with model ages ranging from Paleoproterozoic to Mesoproterozoic and chemical features similar to those of the high-K calc-alkaline series;
- Cariris Velhos granites (Tonian), presenting Mesoproterozoic model ages and chemical characteristics ranging from alkali-rich to calc-alkaline. This group includes Lobo (974 ± 8 Ma) and Rocinha (956 ± 2 Ma) orthogneisses;
- Paleoproterozoic granites from PEAL, with model ages ranging between Neoarchean and Paleoproterozoic and high-K calc-alkaline chemical nature, including Fulgêncio Orthogneiss (1,996 ± 8 Ma);
- Paleoproterozoic granites from RSN, with Archean model ages, mainly represented by Riacho Seco Gneissic-migmatitic Complex (1,992 ± 27 Ma);
- Archean granites from PEAL, represented by rocks of the Entremontes Complex with U-Pb age of 2,734 ± 11 Ma and model age of 3.2 Ga;
- São Francisco Craton granites with model ages ranging from Mesoarchean to Paleoproterozoic periods.

The Orosirian Fulgêncio Orthogneiss is exposed in an extensive area of the domain, and constitutes a very important exposure of older sialic basement rocks in the Western PEAL area. The basement of RSN (subdomain within PEAL) is formed mainly of Archean rocks reworked by Paleoproterozoic tectonic. Data acquired showed that the Western PEAL rocks were affected by four distinct tectonic events, starting with an Archean event, followed by a Paleoproterozoic, and subsequently affected by two others during the Neoproterozoic (Cariris Velhos and Brasiliano Cycle).

ACKNOWLEDGMENTS

The authors are grateful for the reviewers; for the isotope laboratory crew of University of Brasília; for Professor Benjamim Bley Brito Neves due to the geochronological information provided; for the Geologist Andrea Sander because of the great help on description of thin sections; and for the total support provided by the Geological Survey of Brazil (CPRM).

REFERENCES

Almeida F.F.M. 1967. Origem e evolução da plataforma brasileira. Departamento Nacional de Produção Mineral, Mines and Geology Division, *Boletim*, 241, 36 p.

Almeida F.F.M., Hasui Y., Brito Neves B.B., Fuck R.A. 1977. Províncias estruturais brasileiras. *In*: 8º Simpósio de Geologia do Nordeste, Campina Grande. *Resumo das comunicações*. Campina Grande: SBG, 79 p., Boletim Especial SBG, Núcleo Nordeste, 6, p. 12-13.

Almeida F.F.M., Hasui Y., Brito Neves B.B., Fuck R.A. 1981. Brazilian structural provinces: an introduction. *Earth Science Reviews*, **17**:1-29.

Angelim L.A.A., Kosin M. 2001. *Aracaju NW: Folha SC.20-V Estados da Bahia, Pernambuco e Piauí Escala 1:500.000*. Rio de Janeiro, CPRM, 1 CD-Rom, Programa Levantamentos Geológicos Básicos do Brasil.

Bittar S.M.B. 1998. *Faixa Piancó-Alto Brígida: Terrenos tectonoestratigráficos sob regimes metamórficos e deformacionais contrastantes*. Dissertação de Doutorado, Universidade de São Paulo, São Paulo, 126 p.

Bizzi L.A., Schobbenhaus C., Vidotti R.M., Gonçalves J.H. 2003. *Geologia, tectônica e recursos minerais do Brasil: texto, mapas & SIG*. Brasília, Serviço Geológico do Brasil, 692 p.

Boynton W.V. 1984. Cosmochemistry of the rare earth elements: meteorite studies. *In*: Henderson P. (ed.) *Rare Earth Element Geochemistry*, Amsterdam Elsevier, p. 63-114.

Brito M.F.L. & Cruz R.F. 2009. O Complexo Metavulcanossedimentar da região de Salgueiro/PE, Zona Transversal, Província Borborema, NE do Brasil. *In*: SBG, Simpósio de Geologia do Nordeste, 24, 2009. Fortaleza, *Anais...*, 201 p.

Brito M.F.L. & Freitas S. 2011. Caracterização Petrológica e Geotectônica do Ortognaisse Lobo no Domínio Pernambuco-Alagoas, Província Borborema. *In*: 13º Congresso Brasileiro de Geoquímica, *Resumo expandido no Nordeste do Brasil*, Gramado, Rio Grande do Sul.

Brito M.F.L. & Marinho M.S. 2012. *Carta Geológica da Folha Salgueiro SC.24-V-B-III. Estado de Pernambuco*. Recife, CPRM, 2012. 1 mapa, colorido, 91,73 x 69,15 cm. Escala 1:100.000. Programa Geologia do Brasil, In: http://geobank.sa.cprm.gov.br.

Brito Neves B.B. 1983. *O mapa geológico do Nordeste oriental do Brasil, escala 1/1.000.000*. Tese de Livre-Docência, IG/USP, 177 p.

Brito Neves B.B., Santos E.J., Van Schmus W.R. 2000. Tectonic History of the Borborema Province, Northeast Brazil. *In*: Cordani U.G., Milani E.J., Thomaz Filho A., Campos D.A. (eds.) *Tectonic Evolution of South America*, Rio de Janeiro, 31st International Geological Congress, p. 151-182.

Brito Neves B.B., Sial A.N., Rand H.M., Manso V.V. 1982. The Pernambuco- Alagoas Massif, Northeastern Brazil. *Revista Brasileira de Geociências*, **12**:240-250.

Brito Neves B.B., Van Schmus W.R., Santos E.J., Campos Neto M.C. 1995. O Evento Cariris Velhos na Província Borborema; integração de dados, implicações e perspectivas. *Revista Brasileira de Geociências*, **25**(4):279-296.

Caby R., Sial A.N., Arthaud M.H., Vauchez A. 1991. Crustal evolution and the Brasiliano orogeny in northeast Brazil. *In*: Dallmeye R.D., Lécorché J.P. (eds.) *The West African Orogens and Circum-Pacific-Atlantic Correlatives*. Springer-Verlag, Berlin, p. 373-397.

Cruz R.F., Accioly A.C.A. 2013. Petrografia, geoquímica e idade U/Pb do Ortognaisse Rocinha, no Domínio Pernambuco-Alagoas W da Província Borborema. *Estudos Geológicos*, **23**(2):3-27.

Cruz R.F. 2013. Complexo entremontes, remanescente de embasamento arqueano no domínio Pernambuco-Alagoas W da província Borborema. *In*: XVI SNET – Simpósio Nacional de Estudos Tectônicos – Chapada dos Guimarães, Brasil, *Expanded resume*.

Dantas E.L., Van Schmus W.R., Hackspacher P.C., Brito Neves B.B. 1998. Archean accretion in the São José Campestre Massim, Borborema Province, NE of Brazil. *Revista Brasileira de Geociências*, **28**:221-228.

Dantas E.L., Van Schmus W.R., Hackspacher P.C., Fetter A., Brito Neves B.B., Cordani U.G., Nutman A.P., Williams I.S. 2004. The 3.4–3.5 Ga Sao José do Campestre massif, NE Brazil: remnants of the oldest crust in South America. *Precambrian Research*, **130**:113-137.

De Paolo D.J. 1981. A neodymium and strontium isotopic study of the Mesozoic calc- alkaline granitic batholiths of the Sierra Nevada and Peninsular ranges. *California Journal Geophysical Research*, **86**:10470; 10488.

Eby G.N. 1992. Chemical subdivision of the A-type granitoids: petrogenetic and tectonic implications. *Geology*, **20**:641-644.

Fetter A.H., Van Schmus W.R., Santos T.J.S., Nogueira Neto J.A., Arthaud M.H. 2000. U-Pb and Sm-Nd geochronological constraints on the crustal evolution of basement architecture of Ceará state, NW Borborema province, NE Brazil: implications for the existence of the Paleoproterozoic supercontinent 'Atlantica'. *Revista Brasileira de Geociências*, **30**:102-106.

Frost B.R., Barnes C.G., Collins W.J., Arculus R.J., Ellis D.J., Frost C.D. 2001. A geochemical classification for granitic rocks. *Journal of Petrology*, **42**:2033-2048.

Ganade de Araujo C.E., Cordani U.G., Weinberg R.F., Basei M.A., Armstrong R., Sato K. 2014. Tracing Neoproterozoic subduction in the Borborema Province (NE-Brazil): Clues from U-Pb geochronology and Sr-Nd-Hf-O isotopes on granitoids and migmatites. *Lithos*, vol. 202-203, 2014, p. 167-189.

Gioia S.M.C.L., Pimentel M.M. 2000. The Sm-Nd isotopic method in the Geochronology Laboratory of the University of Brasília. *Anais da Academia Brasileira de Ciências*, **72**:219-245.

Guimarães I.P., Silva Filho A.F. 1998. Sm-Nd and Sr isotopic and U-Pb geochronologic constraints for the evolution of the shoshonitic brasiliano Bom Jardim and Toritama Complexes: evidence for a Transamazonic enriched mantle under Borborema Tectonic Province, Brazil. *International Geology Review*, **40**:500-527.

Guimarães I.P., Van Schmus W.R., Brito Neves B.B., Bittar S.M.B., Silva Filho A.F., Armstrong R. 2012. U-Pb zircon ages of orthogneisses and supracrustal rocks of the Cariris Velhos belt: Onset of Neoproterozoic rifting in the Borborema Province, NE Brazil. *Precambrian Research*, 192-195:52-77.

Jardim De Sá E.F. 1994. *A Faixa Seridó (Província Borborema, NE do Brasil) e o seu significado geodinâmico na Cadeia Brasiliana/ Pan-Africana*. Tese de Doutorado, Instituto de Geociências, Universidade de Brasília, 803 p.

Kozuch M. 2003. *Isotopic and Trace Element Geochemistry of Early Neoproterozoic Gneissic and Metavolcanic Rocks in the Cariris Velhos Orogen of the Borborema Province, Brazil, and Their Bearing on Tectonic Setting*. PhD thesis, University of Kansas. 199 p.

Lerouge C., Cocherie A., Toteu S.F., Penaye J., Milesi J.P., Tchameni R. 2006. Shrimp U-Pb zircon age evidence for Paleoproterozoic sedimentation and 2.05 Ga syntectonic plutonism in the Nyong Group, South Western Cameroon: consequences for the Eburnean-Transamazonian belt of NE Brazil and Central Africa'. *Journal of African Earth Sciences*, vol. 44, pp. 413-427.

Ludwig K.R. 2000. Decay constant errors in U–Pb concordia-intercept ages. *Chemical Geology*, **166**:315-318.

Mascarenhas J.F., Garcia T.W. 1989. M*apa geocronológico do Estado da Bahia. Escala 1:1.000.000*. Texto explicativo. Salvador, SME/Superintendência de Geologia e Recursos Minerais, 186 p.

Medeiros V.C. 2000. *Aracaju NE: folha SC.24-X estados da Paraíba, Pernambuco, Alagoas, Sergipe e Bahia. Escala 1:500.000*. Brasília, CPRM, 1 CD-ROM; mapas. Programa Levantamentos Geológicos Básicos do Brasil – PLGB.

Medeiros V.C. 2004. *Evolução geodinâmica e condicionamento estrutural dos terrenos Piancó-Alto Brígida e Alto Pajeú, Domínio da Zona Transversal, NE do Brasil*. Natal. Tese de Doutorado, PPGG, Universidade Federal do Rio Grande do Norte, 200 p.

Medeiros V.C., Santos E.J. 1998. *Folha Garanhuns (SC.24-X-B, escala 1:250.000)*. Integração Geológica (Relatório Interno), CPRM. Recife, Pernambuco, Brazil.

Neves S.P. 2003. Proterozoic history of the Borborema Province (NE Brazil): correlations with neighboring cratons and Pan-African belts, and implications for the evolution of western Gondwana. *Tectonics*, **22**:10-31.

Neves S.P., Lages G.A., Brasilino R.G., Miranda A.W.A. 2014. Paleoproterozoic accretionary and collisional processes and the built-up of the Borborema Province (NE Brazil): geochronological and geochemical evidence from the Central Domain. *Journal of South American Earth Sciences*, doi: 10.1016/j.jsames.2014.06.009.

Neves S.P., Vauchez A., Feraud G. 2000. Tectono-thermal evolution, magma emplacement, and shear zone development in the Caruaru area (Borborema Province, NE Brazil). *Precambrian Research*, **99**:1-32.

Neves S.P., Bruguier O., Vauchez A., Bosch D., Silva J.M.R., Mariano G. 2006. Timing of crust formation, deposition of supracrustal sequences, and Transamazonian and Brasiliano metamorphism in the East Pernambuco belt (Borborema Province, NE Brazil): Implications for western Gondwana assembly. *Precambrian Research*, **149**:197-216.

Oliveira E.P., Toteu S.F., Araújo M.N.C., Carvalho M.J., Nascimento R.S., Bueno J.F., McNaughton N., Basilici G. 2006. Geologic correlation between the Neoproterozoic Sergipano belt (NE Brazil) and the Yaoundé belt (Cameroon, Africa). *Journal of African Earth Sciences*, **44**:470-478.

Pearce J.A. 1996. *Sources and settings of granitic rocks*. Episodes, p. 120-125.

Pearce J.A., Harris N.W., Tindle A.G. 1984. Trace element discrimination diagrams for the tectonic interpretation of granitic rocks. *Journal of Petrology*, **25**:956-983.

Santos E.J. 1995. *O complexo granítico Lagoa das Pedras: acresção e colisão na região de Floresta (Pernambuco), Província Borborema*. Tese de doutorado, Instituto de Geociências, Universidade de São Paulo, São Paulo, 219 p.

Santos E.J., Brito Neves B.B., Van Schmus W.R., Oliveira R.G., Medeiros V.C. 2000. An overall view on the displaced terrane arrangement of the Borborema Province, NE-Brazil. *In*: 31st International Geological Congress, 2000, Rio de Janeiro. *Proceedings*, CD-ROM.

Santos E.J., Nutman A.P., Brito Neves B.B. 2004. Idades SHRIMP U-Pb do Complexo Sertânia: implicações sobre a evolução tectônica da zona transversal, Província Borborema. *Geologia USP*, Série Científica **4**:1-12.

Santos E.J., Van Schmuss W.R., Kozuch M., Brito Neves B.B. 2010. The Cariris Velhos tectonic event in northeast Brazil. *Journal of South American Earth Sciences*, **29**:61-76.

Shand S.J. 1943. *Eruptive Rocks*. Their Genesis, Composition, Classification, and Their Relation to Ore-Deposits with a Chapter on Meteorite. New York, John Wiley & Sons.

Sial A.N. 1986. Granite-types in northeast Brazil: current knowledge. *Revista Brasileira de Geociências*, **16**:54-72.

Silva L.C., Armstrong R., Noce C.M., Carneiro M.A., Pimentel M.M., Pedrosa-Soares A.C., Leite C.A., Vieira V.S., Silva M.A., Castro Paes V.J., Cardoso Filho J.M. 2002. Reavaliação da evolução geológica em terrenos Pré-cambrianos brasileiros com base em novos dados U-Pb Shrimp, Parte I: Províncias Borborema, Mantiqueira Meridional E Rio Negro-Juruena. *Revista Brasileira de Geociências*, **32**(4):529-544.

Silva Filho A.F., Guimarães I.P., Van Schmus W.R. 2002. Crustal evolution of the Pernambuco-Alagoas complex, Borborema province, NE Brazil: Nd isotopic data from Neoproterozoicgranitoids. *Gondwana Research*, **5**:409-422.

Silva Filho A., Guimarães I., Ferreira V.P., Armstrong R., Sial A.N. 2010. Ediacaran Águas Belas pluton, Northeastern Brazil: Evidence on age, emplacement and magma sources during Gondwana amalgamation. *Gondwana Research*, **17**:676-687.

Shand S.J. (1943). *Eruptive Rocks*. Their Genesis, Composition, Classification, and Their Relation to Ore-Deposits with a Chapter on Meteorite. New York: John Wiley & Sons.

Souza Z.S., Martin H., Peucat J.J., Sá E.F.J., Macedo M.H.F. 2007. Calc-alkaline magmatism at the Archean-Proterozoic transition: the Caicó Complex Basement (NE Brazil). *Journal of Petrology*, **48**:2149-2185.

Teixeira L.R. 1997. *O Complexo Caraíba e a Suíte São José do Jacuípe no Cinturão Salvador-Curaçá (Bahia, Brasil): Petrologia, Geoquímica e Potencial Metalogenético*. PhD thesis, Universidade Federal da Bahia, Salvador, 202 p.

Teixeira J.B.G., Silva M.G., Misi A., Cruz S.C.P., Sá J.H.S. 2010. Geotectonic setting and metallogeny of the northern São Francisco craton, Bahia, Brazil. *Journal of South American Earth Sciences*, **30**(15):71-83.

Trompette R. 1994. *Geology of Western Gondwana (2000-500 Ma)*. Balkema, Rotterdan, 350 p.

Van Schmus W.R., Brito Neves B.B., Hackspacher P., Babinski M. 1995. U/Pb and Sm/Nd geochronolgic studies of eastern Borborema Province, Northeastern Brazil: initial conclusions. *Journal of South American Earth Sciences*, **8**:267-288.

Van Schmus W.R., Oliveira E.P., Silva Filho A.F., Toteu F., Penaye J., Guimarães I.P. 2008. *Proterozoic Links between the Borborema Province, NE Brazil, and the Central African Fold Belt* v. 294. Geological Society, London, Special Publication, p. 69-99.

Van Schmus W.R., Kozuch M., Brito Neves B.B. 2011. Precambrian history of the Zona Transversal of the Borborema Province, NE Brazil: Insights from Sm-Nd and U-Pb geochronology. *Journal of South American Earth Sciences*, **31**:227-252.

Vauchez A., Neves S.P., Caby M., Corsini M., Egydio Silva M., Arthaud M.H., Amaro V. 1995. The Borborema shear zone system, NE Brazil. *Journal of South American Earth Sciences,* **8**:247-266.

Wood D.A., Joron J.L., Treuil M.A. 1979. Reappraisal of the use of trace elements to classify and discriminate between magma series erupted in different tectonic settings. *Earth and Planetary Science Letters*, **45**:326-336.

Arquivo digital disponível on-line no site www.sbgeo.org.br